Article

Cell Reports

Macrophage β2-Integrins Regulate IL-22 by ILC3s and Protect from Lethal *Citrobacter rodentium*-Induced Colitis

Graphical Abstract

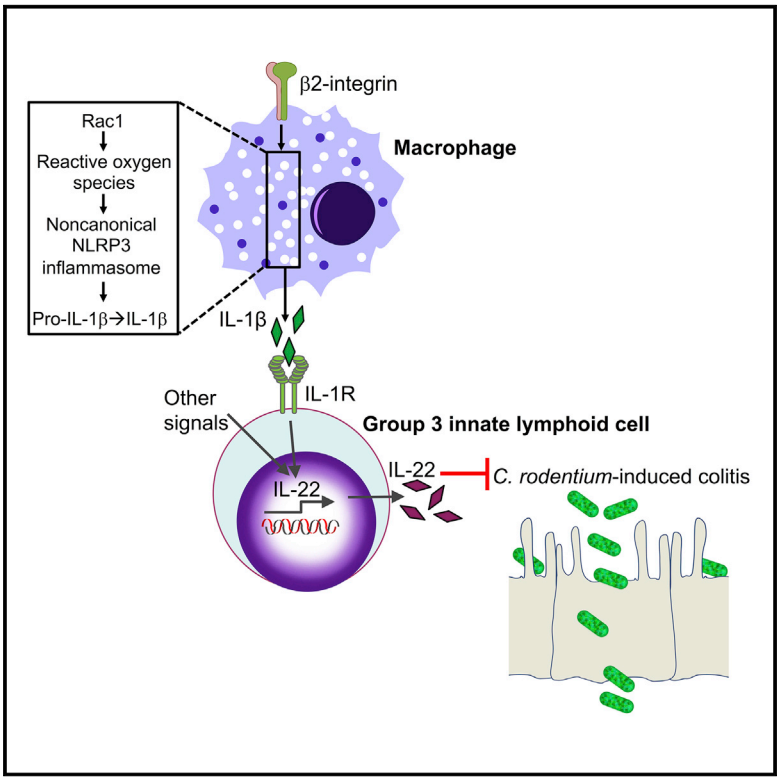

Authors

Baomei Wang, Jong-Hyung Lim, Tetsuhiro Kajikawa, ..., Niki M. Moutsopoulos, Triantafyllos Chavakis, George Hajishengallis

Correspondence

baomei.wang@pennmedicine.upenn.edu (B.W.), geoh@upenn.edu (G.H.)

In Brief

Wang et al. show that β2-integrin expression on intestinal macrophages is required for Rac1/ROS-mediated induction of noncanonical-NLRP3 inflammasome-dependent IL-1β production, which in turn promotes ILC3-derived IL-22. Reduced production of IL-22 due to β2-integrin deficiency in mice causes lethal *C. rodentium* colitis.

Highlights

- β2-integrin deficiency causes lethal *C. rodentium* (CR) colitis in mice
- This phenotype is not attributed to defective neutrophil recruitment
- CR colitis due to β2-integrin deficiency is linked to defective IL-22 responses
- Macrophage β2-integrins are required for IL-1β-dependent induction of IL-22 by ILC3s

Wang et al., 2019, Cell Reports *26*, 1614–1626
February 5, 2019
https://doi.org/10.1016/j.celrep.2019.01.054

CellPress

OPEN ACCESS
CellPress

Cell Reports
Article

Macrophage β2-Integrins Regulate IL-22 by ILC3s and Protect from Lethal *Citrobacter rodentium*-Induced Colitis

Baomei Wang,[1,*] Jong-Hyung Lim,[1,5] Tetsuhiro Kajikawa,[1,5] Xiaofei Li,[1] Bruce A. Vallance,[2] Niki M. Moutsopoulos,[3] Triantafyllos Chavakis,[4] and George Hajishengallis[1,6,*]

[1]Department of Microbiology, University of Pennsylvania School of Dental Medicine, Philadelphia, PA 19104, USA
[2]Department of Pediatrics, Division of Gastroenterology, University of British Columbia, Vancouver, BC V6H 3N1, Canada
[3]Oral Immunity and Inflammation Unit, NIDCR, NIH, Bethesda, MD 20892, USA
[4]Faculty of Medicine, Institute for Clinical Chemistry and Laboratory Medicine, Technische Universität Dresden, 01307 Dresden, Germany
[5]These authors contributed equally
[6]Lead Contact
*Correspondence: baomei.wang@pennmedicine.upenn.edu (B.W.), geoh@upenn.edu (G.H.)
https://doi.org/10.1016/j.celrep.2019.01.054

SUMMARY

β2-integrins promote neutrophil recruitment to infected tissues and are crucial for host defense. Neutrophil recruitment is defective in leukocyte adhesion deficiency type-1 (LAD1), a condition caused by mutations in the CD18 (β2-integrin) gene. Using a model of *Citrobacter rodentium* (CR)-induced colitis, we show that CD18$^{-/-}$ mice display increased intestinal damage and systemic bacterial burden, compared to littermate controls, ultimately succumbing to infection. This phenotype is not attributed to defective neutrophil recruitment, as it is shared by CXCR2$^{-/-}$ mice that survive CR infection. CR-infected CD18$^{-/-}$ mice feature prominent upregulation of IL-17 and downregulation of IL-22. Exogenous IL-22 administration, but not endogenous IL-17 neutralization, protects CD18$^{-/-}$ mice from lethal colitis. β2-integrin expression on macrophages is mechanistically linked to Rac1/ROS-mediated induction of noncanonical-NLRP3 (nucleotide-binding domain, leucine-rich-containing family, pyrin domain-containing-3) inflammasome-dependent IL-1β production, which promotes ILC3-derived IL-22. Therefore, β2-integrins are required for protective IL-1β-dependent IL-22 responses in colitis, and the identified mechanism may underlie the association of human LAD1 with colitis.

INTRODUCTION

Leukocyte adhesion deficiency type 1 (LAD1) is an autosomal recessive primary immunodeficiency caused by mutations in the *ITGB2* gene that encodes the common CD18 subunit of β2-integrins. As β2-integrins are required for firm endothelial adhesion and subsequent transmigration of neutrophils to sites of infection or inflammation, the absence or diminished expression of CD18 in affected individuals results in few or no neutrophils in peripheral tissues (Moutsopoulos et al., 2014; Schmidt et al., 2013). LAD1 patients typically display recurrent bacterial infections and pathological inflammation, primarily in the skin and mucosal surfaces (Hanna and Etzioni, 2012; Moutsopoulos et al., 2014). Gastrointestinal complications and colitis have also been reported in a subset of LAD1 patients (D'Agata et al., 1996; Hawkins et al., 1992; Uzel et al., 2001). However, the mechanism or mechanisms by which β2-integrin deficiency may predispose to LAD1-associated colitis remain uncertain, as does the ability of LAD1 patients to cope with gastrointestinal pathogens.

Similar to human LAD1 patients (Hanna and Etzioni, 2012; Moutsopoulos et al., 2014, 2017), mice with a null mutation in CD18 (CD18$^{-/-}$) have defective neutrophil adhesion and extravasation, have exaggerated interleukin (IL)-17 production in peripheral tissues, and develop skin ulcerations (Scharffetter-Kochanek et al., 1998; Stark et al., 2005). In this study, we used CD18$^{-/-}$ mice in a model of *Citrobacter rodentium*-induced colitis (Koroleva et al., 2015) to gain insights into the potential connection between β2-integrin expression and control of intestinal infection and colitis. *C. rodentium* is a natural Gram-negative enteric pathogen of mice and has been used to model several human intestinal disorders, including Crohn disease and ulcerative colitis (Koroleva et al., 2015). In this regard, *C. rodentium* breaches the intestinal epithelial barrier, leading to a vigorous inflammatory response and colitis. *C. rodentium*-induced colitis is tolerated and resolved in immunocompetent hosts (e.g., wild-type C57BL/6 mice), whereas specific immunodeficiencies lead to varying degrees of susceptibility (Koroleva et al., 2015). For instance, IL-22-deficient (IL-22$^{-/-}$) mice are extremely sensitive and die of *C. rodentium* infection (Zheng et al., 2008). In this regard, early induction of colonic IL-22 upon *C. rodentium* challenge is critical for host protection, and group 3 innate lymphoid cells (ILC3s) are a major source of this protective cytokine (Cella et al., 2009; Sonnenberg et al., 2011; Zheng et al., 2008). Macrophage-derived IL-1β and dendritic cell-derived IL-23 are key cytokines that support the ILC3

expression of IL-22 in the colon (Longman et al., 2014; Manta et al., 2013; Seo et al., 2015).

Here, we show that β2-integrins are required for protection against *C. rodentium*-induced colitis and mortality through a mechanism that is largely independent of defective neutrophil recruitment. Specifically, our findings indicate a role for macrophage β2-integrins in promoting IL-1β release, which subsequently regulates protective ILC3 function. Unlike β2-integrin-sufficient littermates ($CD18^{+/+}$ and $CD18^{+/-}$), $CD18^{-/-}$ mice succumbed to *C. rodentium*-induced colitis in concert with the pronounced upregulation of IL-17 and downregulation of IL-22 as compared to littermate controls. Administration of exogenous IL-22, but not neutralization of endogenous IL-17, protected $CD18^{-/-}$ mice from *C. rodentium*-induced lethal colitis. Mechanistic studies established a role for β2-integrins in macrophages for Rho-family guanosine triphosphatase (GTPase) Rac1 activation, reactive oxygen species (ROS) production, and subsequent induction of noncanonical NLRP3 (nucleotide-binding domain, leucine-rich–containing family, pyrin domain–containing-3) inflammasome-dependent IL-1β release, which in turn promoted a protective ILC3-mediated IL-22 response. In conclusion, we established a transcellular β2 integrin-IL-1β–IL-22 pathway, which mediates protection against *C. rodentium*-induced colitis in mice and suggests a potential link between human LAD1 and susceptibility to colitogenic bacteria.

RESULTS

$CD18^{-/-}$ Mice Are Highly Susceptible to *C. rodentium*-Induced Colitis

The contribution of β2-integrins to gut homeostasis and immunity is poorly characterized, although CD18 deficiency upregulates IL-17 in the intestine and mesenteric lymph nodes (MLNs) in the absence of infection (Stark et al., 2005). However, whether the dysregulated IL-17 response associated with LAD1 causes immunopathology in the gut (as is the case with oral mucosal or skin tissue [Moutsopoulos et al., 2014, 2017]) has not been addressed. Examination of 8-week-old $CD18^{-/-}$ mice showed that they maintain normal weight and colon length (Figures S1A and S1B), although they exhibit splenomegaly relative to CD18-sufficient ($CD18^{+/+}$ and $CD18^{+/-}$) littermates (Figure S1C), as reported earlier (Scharffetter-Kochanek et al., 1998). Histological examination of the $CD18^{-/-}$ colon and cecum revealed normal tissue morphology as compared with that of littermate controls (Figures S1D and S1E). Similarly, when examined at 18 weeks of age, $CD18^{-/-}$ mice were still found to maintain normal colon length and had no signs of colitis (Figures S1F and S1G).

We next addressed whether CD18 deficiency causes increased susceptibility to *C. rodentium*-induced colitis (Koroleva et al., 2015). To this end, $CD18^{-/-}$ mice and littermate controls were orally gavaged with 5×10^8 colony-forming units (CFUs) of *C. rodentium*. $CD18^{+/+}$ and $CD18^{+/-}$ littermates were able to survive the infection (Figure 1A) without significant changes in body weight (Figure 1B). In stark contrast, $CD18^{-/-}$ mice suffered a significant drop in body weight from day 5 onward (Figure 1B) and rapidly succumbed to infection, starting at day 8 and leading to 100% mortality by day 12 (Figure 1A). Fluorescence *in situ* hybridization showed that as early as day 5 post-infection, $CD18^{-/-}$ mice exhibited markedly elevated *C. rodentium* burdens (as compared to $CD18^{+/-}$ mice) within the distal colon adjacent to or associated with the intestinal epithelial cells (Figure 1C). In the same time interval, $CD18^{-/-}$ mice displayed a marked dissemination of *C. rodentium* to peripheral organs, including MLNs, spleens, and livers, whereas in $CD18^{+/-}$ controls, *C. rodentium* bacteria were barely detectable in these organs, despite their abundance in the feces (Figure 1D). Moreover, the pronounced susceptibility of $CD18^{-/-}$ mice was associated with a significant reduction in colon length (a marker of colitis) at day 8 post-infection (Figure 1E) and with concomitantly increased *C. rodentium* bacterial burdens in the spleens and livers (Figure 1F), as compared to CD18-sufficient littermates. In addition, histological analysis revealed cecal and colonic mucosa hyperplasia and ulceration in *C. rodentium*-infected $CD18^{-/-}$ mice (Figure 1G), thereby resulting in significantly higher cecal and colonic histopathology scores relative to their CD18-sufficient littermate controls (Figure 1H). Therefore, in the setting of CD18 deficiency, *C. rodentium* causes increased intestinal epithelial damage, systemic pathogen burdens, and mortality in mice during infection with *C. rodentium*.

Differential Regulation of IL-17 and IL-22 in $CD18^{-/-}$ Large Intestine after *C. rodentium* Infection

Neutrophils in $CD18^{-/-}$ mice show defective extravasation and recruitment to sites of infection or inflammation (Scharffetter-Kochanek et al., 1998). Consistent with this, flow cytometric analysis revealed significantly reduced neutrophil infiltration on day 8 post-infection in the colonic lamina propria of $CD18^{-/-}$ mice as compared to their $CD18^{+/-}$ littermate controls (Figure S2A). As β2-integrins mediate multiple functions besides neutrophil recruitment, we used mice deficient in C-X-C motif chemokine receptor 2 ($CXCR2^{-/-}$) to determine the importance of recruited neutrophils in *C. rodentium*-induced colitis. CXCR2 is a major chemokine receptor expressed on neutrophils, and $CXCR2^{-/-}$ mice display few or no neutrophils in the colon and other sites of infection due to defective neutrophil chemotaxis (Spehlmann et al., 2009; Zenobia et al., 2013), as also confirmed in our study (Figure S2B**)**. Upon oral gavage with *C. rodentium*, all $CXCR2^{-/-}$ mice survived the infection, whereas all $CD18^{-/-}$ mice (infected in a side-by-side experiment) died by day 12 (Figure S2C). $CXCR2^{-/-}$ mice maintained normal body weight and colon length (Figures S2D and S2E), although they exhibited modestly increased bacterial loads within systemic tissues as compared to $CXCR2^{+/+}$ littermate controls (differences reached statistical significance in spleens but not in livers; Figure S2F). Histologically, $CXCR2^{-/-}$ mice displayed increased colonic inflammation, edema, and epithelial damage (Figure S2G) and modestly higher colonic pathology scores relative to $CXCR2^{+/+}$ controls (Figure S2H). These data suggest that the lethal *C. rodentium*-induced colitis seen in $CD18^{-/-}$ mice during the second week post-infection cannot be adequately explained by defects in neutrophil recruitment.

We thus next investigated alternative mechanisms underlying the increased susceptibility of $CD18^{-/-}$ mice to *C. rodentium*-induced colitis. To this end, we examined their colonic cytokine expression profile at day 5 post-infection—in other words, just before the time that $CD18^{-/-}$ mice started losing significant

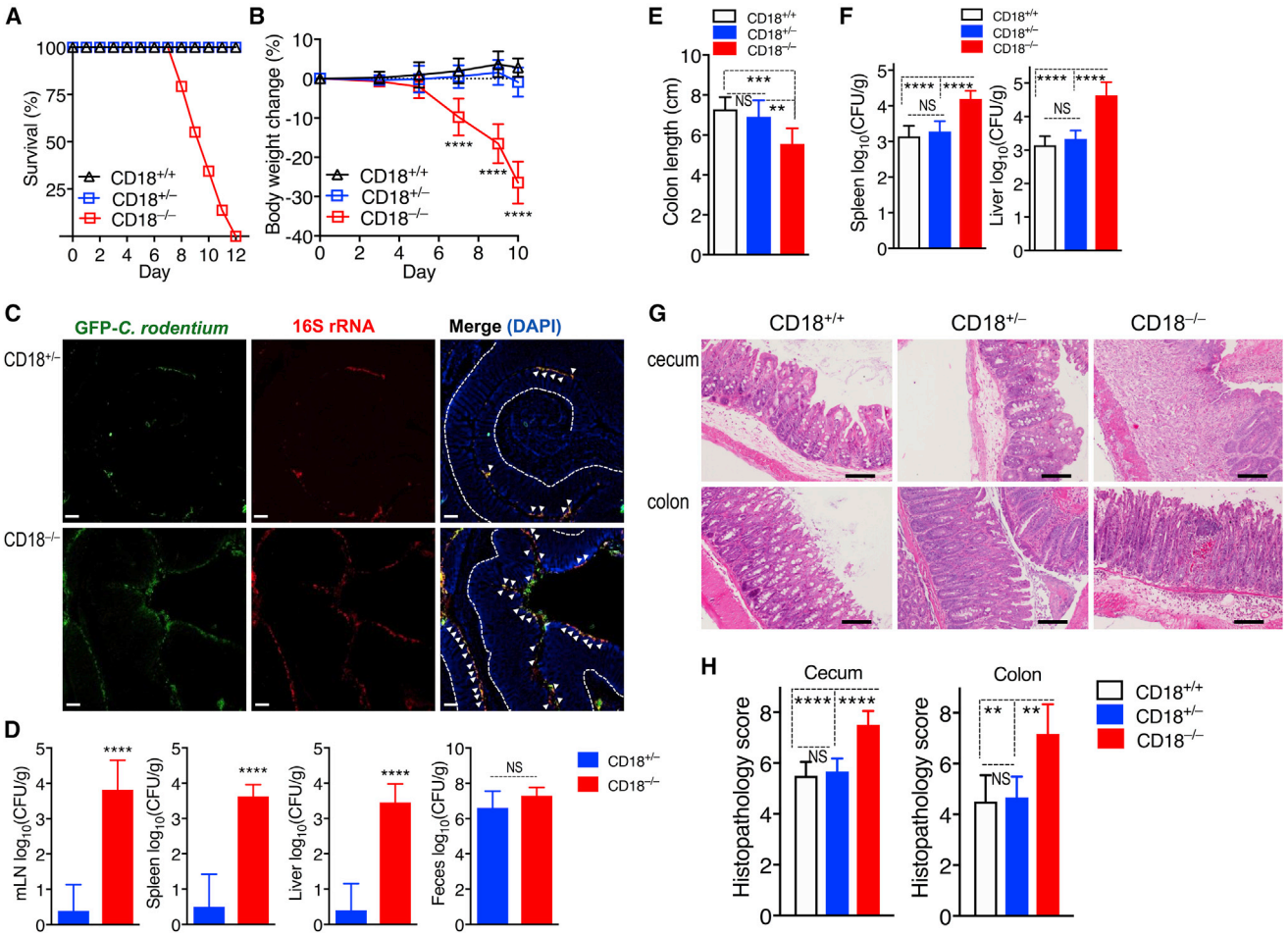

Figure 1. CD18 Deficiency Renders Mice Highly Susceptible to *C. rodentium*-Induced Colitis

(A and B) Survival rates (A) and average weight changes (B) at the indicated time points in CD18$^{-/-}$, CD18$^{+/-}$, and CD18$^{+/+}$ littermates orally inoculated with *C. rodentium* at the age of 8 weeks.

(C and D) CD18$^{-/-}$ and CD18$^{+/-}$ mice were orally inoculated with GFP-expressing and antibiotic-resistant *C. rodentium*, and after 5 days, tissues were harvested to visualize bacteria by fluorescence *in situ* hybridization (FISH) and determine bacterial load.

(C) Colon sections from CD18$^{-/-}$ and CD18$^{+/-}$ littermates were stained with a universal probe that targets the 16S rRNA gene of all bacteria (red) and anti-GFP antibody (green). Sections were counterstained with DAPI to visualize nuclei. Scale bars, 50 μm. Dotted line indicates basement membrane and arrowheads indicate bacteria associated with the distal colonic epithelium.

(D) Log_{10} CFU of *C. rodentium* in MLNs, spleens, livers, and feces.

(E–H) CD18$^{-/-}$, CD18$^{+/-}$ and CD18$^{+/+}$ mice were orally inoculated with *C. rodentium*, and after 8 days, tissues were harvested to determine (E) colon length and (F) log_{10} CFU of *C. rodentium* in spleen and liver. (G) H&E-stained cecum and colon sections (scale bars, 100 μm) and (H) histopathology scores of cecum and colon sections at day 8 post-infection.

Numerical data are means ± SDs and are pooled from 4 independent experiments with 7–8 mice/group in each experiment, for a total of 29 mice/group (A); are from 2 independent experiments with 3 mice/group, for a total of 6 mice/group (B and F); are from 2 independent experiments with 4–5 mice/group, for a total of 8–9 mice/group (D and E); or are from 2 independent experiments with 3 mice/group, for a total of 6 mice/group (H). Images are representative of 2 independent experiments with 3–4 mice/group (C and G). **p < 0.01, ***p < 0.001, and ****p < 0.0001 (B: 2-way ANOVA with repeated-measures and Dunnett's multiple-comparisons test; D: 2-tailed Student's t test; E, F, and H: or 1-way ANOVA with Tukey's multiple-comparisons test). NS, non-significant.

weight and began to succumb to infection. Similar to the IL-17-dominated gene expression signature seen in human and murine oral mucosal tissues in the setting of LAD1-associated periodontitis (Moutsopoulos et al., 2014, 2017), *C. rodentium* infection of CD18$^{-/-}$ mice elicited significantly higher mRNA expression of IL-17 (although not of tumor necrosis factor [TNF] or IL-6) as compared to the CD18-sufficient (CD18$^{+/-}$) littermate controls, which also showed elevated IL-17 mRNA expression relative to pre-infection baseline levels (Figure 2A). In stark contrast to IL-17, the mRNA expression of IL-22 and of IL-22-dependent antimicrobial genes (Reg3β and Reg3γ) was markedly reduced (compared to littermate controls) in the CD18$^{-/-}$ colon (Figure 2A). The differentially regulated expression of IL-17 and IL-22 in the *C. rodentium*-infected CD18$^{-/-}$ colon was confirmed at the protein level (Figure 2B). These data suggest that colonic IL-22 expression is under β2-integrin regulation.

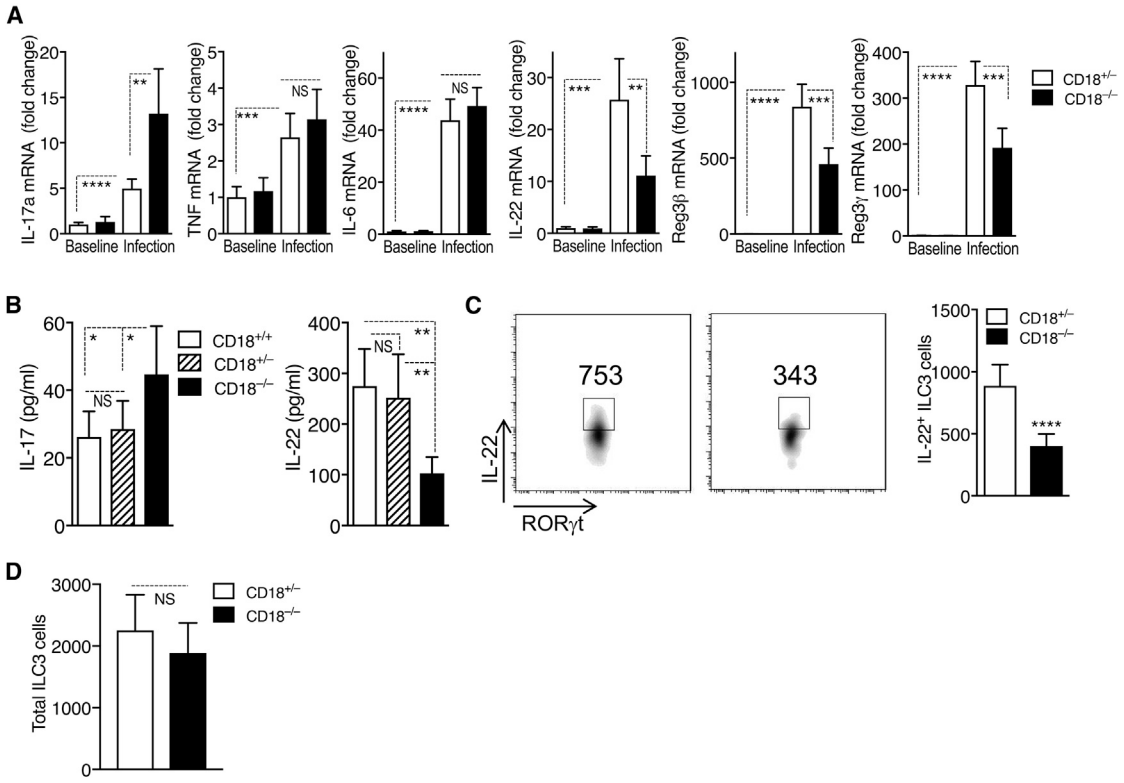

Figure 2. Differential Regulation of IL-17 and IL-22 in CD18$^{-/-}$ Colon after *C. rodentium* Infection

(A and B) Eight-week-old CD18$^{-/-}$ mice and CD18-sufficient littermate controls (CD18$^{+/-}$ and/or CD18$^{+/+}$) were orally inoculated with *C. rodentium*. On day 5, colonic tissue was harvested, and expression of the indicated cytokines was determined (A) at the mRNA level by quantitative real-time PCR and (B) at the protein level by *ex vivo* colon culture ELISA.

(C and D) On day 5 post-infection, LPMCs were isolated from the large intestine of CD18$^{-/-}$ or CD18$^{+/-}$ mice and analyzed by flow cytometry for IL-22$^+$ ILC3 cells (shown are representative fluorescence-activated cell sorting [FACS] plots [left] and absolute numbers [right] of IL-22-expressing RORγt$^+$ ILCs [gated on CD3$^-$CD5$^-$B220$^-$NK1.1$^-$F4/80$^-$Gr-1$^-$CD127$^+$CD90.2$^+$RORγt$^+$]) (C) and for total number of ILC3 cells (D).

Data are means ± SDs and are pooled from 2 independent experiments with 3 mice/group in each experiment, for a total of 6 mice/group (A and B); are from 2 independent experiments with 3 mice/group in one experiment and 4 mice/group in the second experiment, for a total of 7 mice/group (C); or are from 3 independent experiments with 3 mice/group in each experiment, for a total of 9 mice/group (D). *p < 0.05, **p < 0.01, ***p < 0.001, and ****p < 0.0001 (A, C, and D: 2-tailed Student's t test; B: or 1-way ANOVA with Tukey's multiple-comparisons test). NS, non-significant.

Compared to their littermate controls, *C. rodentium*-infected CD18$^{-/-}$ mice exhibited markedly increased numbers of γδ T cells in the lamina propria of the large intestine, MLNs, and spleens (Figure S3A) and a significantly higher frequency of IL-17-expressing γδT cells in the same tissues (Figure S3B). As ILC3s constitute the predominant source of IL-22 in the early stage of *C. rodentium* infection (Sonnenberg and Artis, 2015), we examined the numbers of IL-22-expressing ILC3s in the large intestinal lamina propria on day 5 post-infection. The analysis revealed a significant reduction in the numbers of IL-22$^+$ ILC3s in CD18$^{-/-}$ mice as compared to those in CD18$^{+/-}$ littermate controls (Figures 2C and S4A). In contrast, there were no significant differences between CD18$^{-/-}$ and CD18$^{+/-}$ mice regarding the total number of ILC3 cells (Figure 2D). Therefore, the reduced numbers of IL-22$^+$ ILC3 cells was not the result of a reduction in the total ILC3 cell numbers, but is likely attributable to the defective regulation of IL-22 induction in ILC3s. These findings collectively indicate that in the absence of β2-integrin expression, *C. rodentium* causes a pronounced dysregulation of intestinal IL-17 and IL-22 responses.

Although IL-22-expressing CD4 T cells are important for immunity against *C. rodentium* at later stages of infection (mice lacking T cells start dying after the second week of infection) (Basu et al., 2012; Sonnenberg et al., 2011; Vallance et al., 2002), we examined whether CD18 deficiency could also affect IL-22 production by T cells at a relatively early stage that is relevant to our study model. On day 8 post-infection, we isolated total lamina propria mononuclear cells (LPMCs) from the colons of *C. rodentium*-infected CD18$^{-/-}$ and CD18$^{+/-}$ mice and quantified the numbers of IL-22-producing CD4 T cells by flow cytometry. Although T cell-derived IL-17 could be readily detected at this time point, T cell-derived IL-22 was not detectable in the colons of *C. rodentium*-infected CD18$^{-/-}$ or CD18$^{+/-}$ mice (Figure S4B). Thus, the IL-22 defect underlying the pronounced susceptibility of CD18$^{-/-}$ mice to *C. rodentium* infection involves ILC3s and not CD4 T cells.

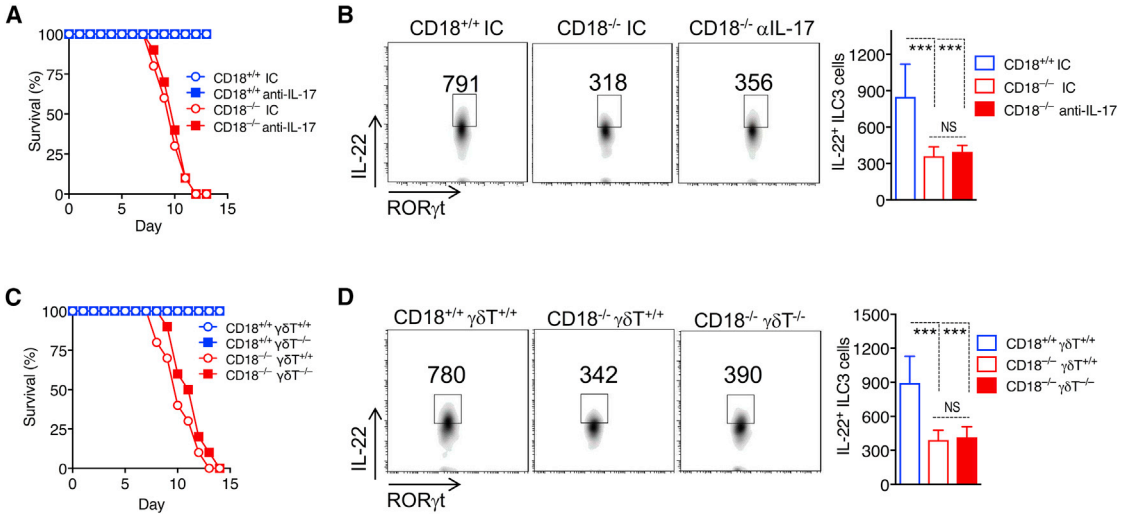

Figure 3. Role of IL-17 and IL-17$^+$γδT Cells in *C. rodentium* Infection of CD18$^{-/-}$ Mice

(A and B) Eight-week-old CD18$^{-/-}$ and CD18$^{+/+}$ littermates were injected intravenously (i.v.) with either anti-IL-17 antibody or isotype control IgG (IC) on a daily basis for 7 days starting 1 day before *C. rodentium* infection.

(A) Survival rates at the indicated time points.

(B) On day 5 post-infection, LPMCs were isolated from the large intestine of the indicated mouse groups and analyzed by flow cytometry; shown are representative FACS plots (left) and absolute numbers (right) of IL-22-expressing RORγt$^+$ ILCs (gated on CD3$^-$CD5$^-$B220$^-$NK1.1$^-$F4/80$^-$Gr-1$^-$CD127$^+$CD90.2$^+$RORγt$^+$).

(C and D) Eight-week-old CD18$^{-/-}$/γδT$^{-/-}$ mice and CD18$^{-/-}$/γδT$^{+/+}$ littermates (as well as CD18-sufficient mice with or without γδ T cell deficiency) were orally inoculated with *C. rodentium*.

(C) Survival rates at the indicated time points.

(D) On day 5 post-infection, LPMCs were isolated from the large intestine of the indicated mouse groups and analyzed by flow cytometry; shown are representative FACS plots (left) and absolute numbers (right) of IL-22-expressing RORγt$^+$ ILCs (gated on CD3$^-$CD5$^-$B220$^-$NK1.1$^-$F4/80$^-$Gr-1$^-$CD127$^+$CD90.2$^+$RORγt$^+$).

Data are means ± SDs and are pooled from 2 independent experiments with 5 mice/group in each experiment, for a total of 10 mice/group (A and C); or are from 2 independent experiments with 3 mice/group, for a total of 6 mice/group (B and D). ***$p < 0.001$ (B and D: 1-way ANOVA with Tukey's multiple-comparisons test). NS, non-significant.

Role of IL-17 and IL-22 in the Protection of CD18$^{-/-}$ Mice against *C. rodentium* Infection

Despite the marked dysregulation of IL-17 and IL-22 due to CD18 deficiency, it was uncertain whether the observed susceptibility to *C. rodentium*-induced colitis of the CD18$^{-/-}$ mice was mediated by their exaggerated IL-17 response, their diminished IL-22 response, or both. Under certain conditions, IL-17 can inhibit the expression of IL-22 and, moreover, may determine the balance between its tissue-protective and its pathological effects (Sonnenberg et al., 2010). To determine the role of IL-17 during *C. rodentium*-induced colitis in the context of β2-integrin deficiency, CD18$^{-/-}$ mice and CD18$^{+/+}$ littermate controls were systemically administered anti-IL-17 neutralizing monoclonal antibody (mAb) or immunoglobulin G1 (IgG1) isotype control, as previously described (Xiong et al., 2016). The anti-IL-17 treatment had no influence on the survival of either genotype (Figure 3A), although, as expected, it reduced the granulocyte-colony-stimulating factor (G-CSF) levels in the blood of treated animals (Figure S4C). Moreover, the inability of anti-IL-17 treatment to extend the survival of CD18$^{-/-}$ mice was associated with the failure to upregulate IL-22 expression by ILC3s in the large intestine (Figure 3B). Furthermore, we induced colitis in CD18$^{-/-}$ mice and CD18$^{-/-}$/γδT$^{-/-}$ mice to determine whether depletion of γδT cells, a major cellular source of intestinal IL-17 in CD18$^{-/-}$ mice (Figures S3A and S3B), would influence the outcome of *C. rodentium*-induced colitis. Similar to the anti-IL-17 treatment, depletion of γδT cells failed to improve or otherwise affect mouse survival (Figure 3C) or IL-22 production by ILC3s (Figure 3D).

To determine whether the diminished IL-22 production in the colon of CD18$^{-/-}$ mice underlies their marked susceptibility to *C. rodentium* infection, we treated *C. rodentium*-infected CD18$^{-/-}$ mice with recombinant IL-22-Fc or IgG control using a previously established approach (Ota et al., 2011). In contrast to control-treated CD18$^{-/-}$ mice that succumbed to infection by day 13 and experienced significant body weight loss from day 6 onward, IL-22-Fc-treated CD18$^{-/-}$ mice were rescued from infection-induced weight loss and lethality (Figures 4A and 4B). Moreover, in comparison to the control treatment, IL-22-Fc treatment significantly reduced the systemic spread of bacteria to the livers and spleens of CD18$^{-/-}$ mice, leaving them with CFU values that are comparable to those of CD18$^{+/+}$ mice (Figure 4C). Histological analysis of the colon consistently showed that the IL-22 treatment reduced epithelial cell damage and clinical scores (Figures 4D and 4E). β2-Integrin deficiency is thus associated with increased numbers of IL-17-producing γδT cells

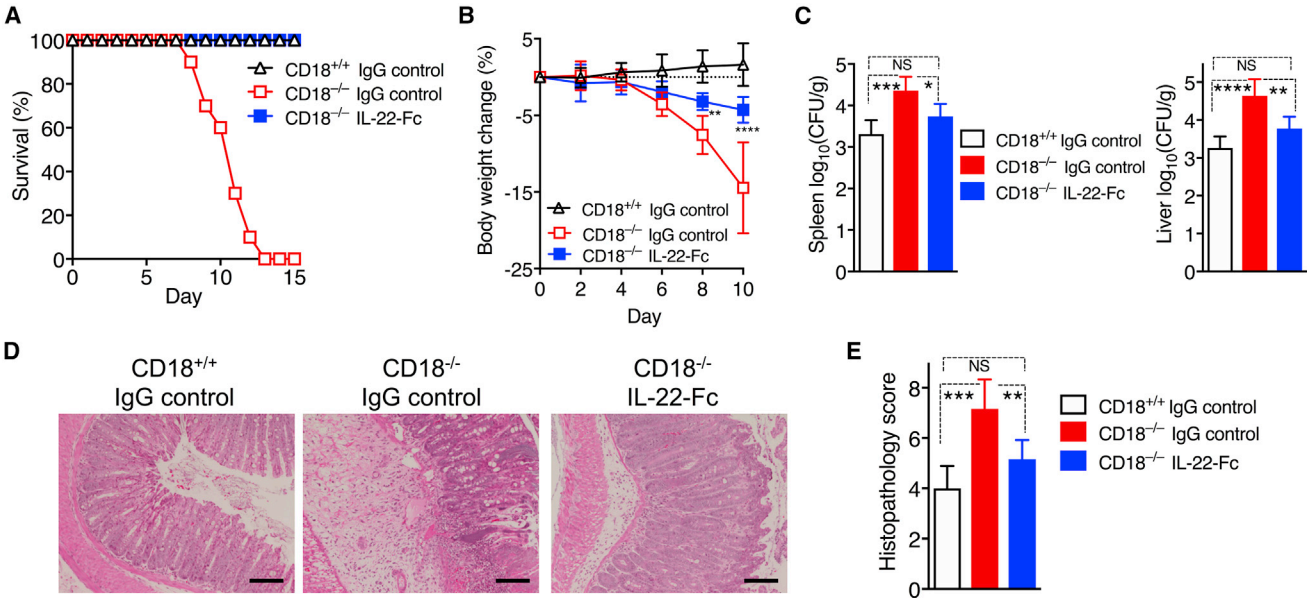

Figure 4. Exogenous IL-22 Protects CD18$^{-/-}$ Mice from *C. rodentium*-Induced Lethality

Eight-week-old CD18$^{-/-}$ and CD18$^{+/+}$ littermates were given i.v. IL-22-Fc or control IgG every 3 days starting on the same day as bacteria inoculation.

(A and B) Survival rates (A) and average weight changes (B) at indicated time points.

(C–E) At day 8 post-infection, tissues were harvested to determine $\log_{10}$ CFU of *C. rodentium* bacteria in spleen and liver (C), perform H&E staining of colon sections (scale bars, 100 μm) (D), and determine histopathology scores of colon sections (E).

Data are means ± SDs and are pooled from 2 independent experiments with 5 mice/group in each experiment, for a total of 10 mice/group (A); are from 2 independent experiments with 4 mice/group, for a total of 8 mice/group (B); or are representative of 2 independent experiments with 3 mice/group, for a total of 6 mice/group (C and E). *p < 0.05, **p < 0.01, ***p < 0.001, and ****p < 0.0001 (B: 2-way ANOVA with repeated-measures and Bonferroni's multiple-comparisons test; C and E: 1-way ANOVA with Tukey's multiple-comparisons test).

and reduced numbers of IL-22-expressing ILC3s in the gut, although only the latter is associated with impaired host protection against *C. rodentium*-induced colitis.

Reduced IL-1β Secretion in CD18$^{-/-}$ Macrophages in Response to *C. rodentium* Infection Impairs ILC3 Production of IL-22

We next examined the possible mechanisms linking β2-integrin deficiency to defective ILC3 production of IL-22. To determine the possibility of cell-intrinsic effects, we compared IL-22 production between CD18$^{-/-}$ and CD18$^{+/-}$ ILC3s after stimulation with IL-1β, IL-23, or both. Our analysis did not reveal inherent defects in CD18$^{-/-}$ ILC3s, as they were able to produce IL-22 and IL-17 at levels similar to those seen in β2-integrin-sufficient (CD18$^{+/-}$) controls (Figure 5A). We thus next investigated potential ILC3-extrinsic factors that were responsible for the impaired production of IL-22 in the CD18$^{-/-}$ colon (Figure 2), such as defective activation of ILC3s by bystander β2-integrin-deficient leukocytes. Specifically, we hypothesized that the impaired production of IL-22 by CD18$^{-/-}$ ILC3s could be attributed to decreased levels of IL-1β and/or IL-23, which are key macrophage- and dendritic cell-derived cytokines supporting ILC3 expression of IL-22 (Longman et al., 2014; Manta et al., 2013; Seo et al., 2015). To this end, we measured these cytokines in colon tissue homogenates on day 5 post-*C. rodentium* infection. The production of IL-23 protein in the colon of CD18$^{-/-}$ mice was not decreased (rather, modestly increased) as compared to that of CD18$^{+/-}$ littermate controls (Figure 5B, left). The production of IL-1β was significantly decreased, thus correlating with the reduced production of IL-22 in the CD18$^{-/-}$ colon (Figure 5B, center and right, respectively). The production of IL-1β was also significantly diminished in *ex vivo* cultures of total LPMCs isolated from the colon of *C. rodentium*-infected CD18$^{-/-}$ mice, as compared to LPMCs from the colons of infected CD18$^{+/-}$ control mice (Figure 5C, left). Therefore, β2-integrins appear to be required for optimal production of leukocyte-derived IL-1β in the colon, although not of leukocyte-derived IL-6 since CD18$^{-/-}$ and CD18$^{+/-}$ LPMCs produced similar amounts of IL-6 (Figure 5C, center). Consistent with the *in vivo* tissue findings, the reduced IL-1β production by CD18$^{-/-}$ LPMCs correlated with the decreased production of IL-22 in the same cultures (relative to their CD18$^{+/-}$ counterparts; Figure 5C, right).

Given that the macrophages in the intestinal lamina propria constitute a major cellular source of IL-1β (Seo et al., 2015), we next investigated whether β2-integrin deficiency could affect the macrophage IL-1β response. To this end, bone marrow-derived macrophages (BMDMs) were stimulated with *C. rodentium*, and cytokine production was measured in culture supernatants. CD18$^{-/-}$ macrophages exhibited significantly decreased production of IL-1β in response to *C. rodentium*, although their ability to produce IL-6 or TNF was similar to that of CD18$^{+/-}$ controls (Figure 5D). Therefore, β2-integrin deficiency selectively impairs IL-1β production in *C. rodentium*-challenged

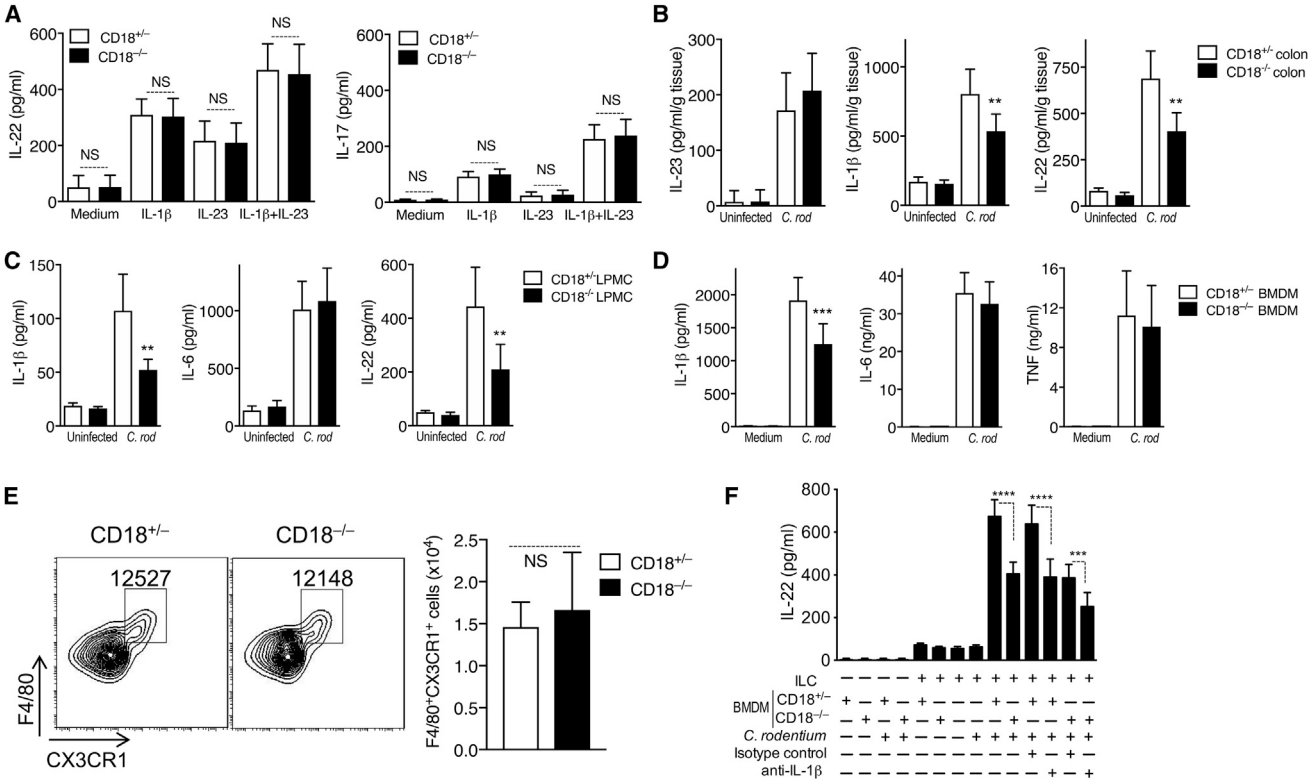

Figure 5. β2-Integrins Regulate Macrophage Production of IL-1β in Response to *C. rodentium* Infection

(A) ILCs ($CD3^-CD5^-B220^-NK1.1^-F4/80^-Gr\text{-}1^-CD90^+CD127^+CD25^+KLRG1^-$) were sort-purified from the intestines of naive $CD18^{+/-}$ or $CD18^{-/-}$ littermates. Sorted ILCs were cultured in 96-well plates in the presence of 20 ng/mL IL-1β, 20 ng/mL IL-23, both IL-1β and IL-23, or in medium only for 72 h. The release of IL-22 (left) and IL-17 (right) in culture supernatants was determined by ELISA.

(B and C) Eight-week-old $CD18^{-/-}$ mice and $CD18^{+/-}$ littermate controls were orally inoculated with *C. rodentium*. On day 5, colons were harvested, and production of the indicated cytokines was determined by ELISA of (B) colonic tissue homogenates and (C) supernatants from *ex vivo* cultures of total large intestinal lamina propria mononuclear cells (LPMCs).

(D) Bone marrow-derived macrophages (BMDMs) were generated from $CD18^{+/-}$ and $CD18^{-/-}$ mice and stimulated with *C. rodentium* (*C. rod*) (MOI 20:1) for 1 h without antibiotics and then cultured for another 17 h with gentamicin (50 μg/mL).

(E) Eight-week-old $CD18^{-/-}$ mice and $CD18^{+/-}$ littermate controls were orally inoculated with *C. rodentium*. On day 5 post-infection, LPMCs were isolated from the large intestine and analyzed by flow cytometry; shown are representative FACS plots (left) and absolute numbers (right) of $F4/80^+CX3CR1^+$ macrophages (gated on $CD45^+CD3^-B220^-NK1.1^-Ly6G^-$).

(F) ILCs ($CD3^-CD5^-B220^-NK1.1^-F4/80^-Gr\text{-}1^-CD90^+CD127^+CD25^+KLRG1^-$) were sort-purified from the intestine of naive $CD18^{-/-}$ mice. Sorted ILCs and BMDMs from naive $CD18^{+/-}$ or $CD18^{-/-}$ mice were cultured alone or co-cultured, with or without stimulation with *C. rodentium* (MOI 20:1) for 24 h, in the presence of neutralizing antibody to IL-1β or isotype control (IC). The indicated cytokines were measured by ELISA of culture supernatants.

Data are means ± SDs and are pooled from 3 independent experiments performed in duplicate, for a total of 6 replicates/group (A); are from 3 independent experiments with 2 mice/group in 2 experiments and 3 mice/group in another, for a total of 7 mice/group (B); are from 2 independent experiments with 3–4 mice/group, for a total of 6–8 mice/group (C); are from 2 independent experiments with 3 mice/group in one experiment and 4 mice/group in the other experiment, for a total of 7 mice/group (E); or are from 3 independent experiments performed in triplicate, for a total of 9 mice/group (D and F). $^{**}p < 0.01$ and $^{***}p < 0.001$ (2-tailed Student's t test). NS, non-significant.

macrophages. We also showed that the numbers of $F4/80^+CX3CR1^+$ macrophages in the colons of $CD18^{-/-}$ and CD18-sufficient ($CD18^{+/-}$) mice were comparable (Figure 5E), thus ruling out the possibility that the reduced production of colonic IL-1β in $CD18^{-/-}$ mice could be attributed, at least in part, to the low abundance of macrophages.

To obtain direct evidence that macrophage CD18 deficiency impairs IL-22 production by $CD18^{-/-}$ ILC3s in an IL-1β-dependent manner, BMDMs and ILC3s were cultured separately or together in the presence or absence of *C. rodentium*. IL-22 production was induced only in the presence of both cell types and concomitant stimulation by *C. rodentium* (Figure 5F). ILC3s produced significantly lower IL-22 when co-cultured with $CD18^{-/-}$ as compared to $CD18^{+/-}$ BMDMs (Figure 5F). However, the ability of $CD18^{+/-}$ BMDMs to support IL-22 production in the co-culture system was significantly inhibited in the presence of neutralizing antibody to IL-1β (Figure 5F). A similar observation was made for co-cultures containing $CD18^{-/-}$ BMDMs, the ability of which to support IL-22 production was reduced even further by anti-IL-1β. In a similar experiment, combined anti-IL-1β and anti-IL-23 treatment did not reduce IL-22 production more than anti-IL-1β treatment alone did (Figure S5), suggesting that

IL-23 is not endogenously produced in the system at levels sufficient to influence IL-22 production. These data indicate that ILC3 production of IL-22 is regulated by β2-integrins on macrophages in a paracrine manner involving macrophage-derived IL-1β secretion.

β2-Integrins Mediate the Activation of the ROS-Noncanonical NLRP3-IL-1β Axis

The production and release of bioactive IL-1β is a multistep, tightly controlled process. It includes pattern recognition receptor-induced mRNA expression and protein synthesis of pro-IL-1β, which is subsequently cleaved by inflammasome-induced caspase-1 into the active and secreted forms of IL-1β (Lamkanfi and Dixit, 2014; Sharma and Kanneganti, 2016). Upon challenge with *C. rodentium*, CD18$^{+/-}$ and CD18$^{-/-}$ BMDMs expressed similar levels of IL-1β mRNA at 8 and 18 h post-challenge (Figure 6A), suggesting that β2-integrins do not regulate macrophage IL-1β mRNA expression in response to this pathogen. We next investigated whether the reduced IL-1β production in *C. rodentium*-challenged CD18$^{-/-}$ BMDMs involved defective inflammasome function. In this regard, Gram-negative enteric pathogens such as *C. rodentium* selectively activate the noncanonical pathway of the NLRP3 inflammasome, which entails the upstream activation of caspase-11 that is crucial for caspase-1 activation and IL-1β production in macrophages (Kayagaki et al., 2011; Rathinam et al., 2012). We confirmed that the inhibition of caspase-11 (with wedelolactone), NLRP3 (with glyburide), or caspase-1 (with N-acetyl-tyrosyl-valyl-alanyl-aspartyl chloromethyl ketone [Ac-YVAD-CMK]) resulted in significantly reduced IL-1β (but not TNF) responses in *C. rodentium*-challenged CD18$^{+/-}$ BMDMs and further diminished the IL-1β levels in CD18$^{-/-}$ BMDMs (without affecting their TNF response) (Figure 6B). The findings that IL-1β production by *C. rodentium*-stimulated BMDMs is regulated by CD18 and the inflammasome pathway were reproduced using similarly treated CD18$^{+/-}$ and CD18$^{-/-}$ intestinal macrophages (CD45^{+}Lin^{-}(CD3NK1.1B220Ly6G)F4/80^{+}CX3CR1^{+}) (Figure S6A). These results validated our *in vitro* BMDM system as biologically relevant for further mechanistic investigations.

Since ROS upregulates caspase-11 expression of the noncanonical NLRP3 inflammasome and promotes IL-1β production in response to *C. rodentium* infection (Lupfer et al., 2014), we examined whether the defect in IL-1β production by *C. rodentium*-infected CD18$^{-/-}$ BMDMs could be attributed to reduced ROS production. *C. rodentium*-challenged CD18$^{-/-}$ BMDMs elicited significantly reduced ROS production relative to similarly treated CD18$^{+/-}$ BMDMs as shown by H2DCFDA staining (Figure 6C), indicating that *C. rodentium*-induced ROS generation is largely dependent on the presence of β2-integrins. Moreover, caspase-11 expression in CD18$^{-/-}$ BMDMs in response to *C. rodentium* was significantly lower than in CD18$^{+/-}$ BMDMs (Figure 6D). The importance of ROS generation for noncanonical NLRP3-dependent IL-1β production in our system was substantiated by showing that treatment of *C. rodentium*-challenged CD18$^{+/-}$ or CD18$^{-/-}$ BMDMs with the ROS scavenger *N*-acetyl-L-cysteine (NAC) significantly reduced caspase-11 expression (Figure 6D) and IL-1β (but not TNF) production (Figure 6E). To further substantiate that the impaired caspase-11 expression in *C. rodentium*-challenged CD18$^{-/-}$ BMDMs results from the reduced generation of ROS, we supplemented the cells with an exogenous source of ROS (H_2O_2). The H_2O_2 treatment restored caspase-11 expression in CD18$^{-/-}$ BMDMs to levels that are comparable to those of untreated (i.e., not given H_2O_2) *C. rodentium*-challenged CD18$^{+/-}$ BMDMs (Figure S6B).

The Rho-family GTPase Rac1 acts downstream of integrins (Nurmi et al., 2007) and is a crucial mediator of ROS production (Heasman and Ridley, 2008). To determine whether the decreased ROS production in CD18$^{-/-}$ BMDMs (Figure 6C) is linked to defective Rac1 activation, we assessed Rac1 activity in *C. rodentium*-infected CD18$^{-/-}$ and CD18$^{+/-}$ BMDMs. CD18$^{-/-}$ BMDMs exhibited significantly reduced levels of Rac1 activity upon *C. rodentium* infection as compared to CD18$^{+/-}$ BMDMs (Figure 6F). Moreover, the ability of CD18$^{+/-}$ BMDMs to produce ROS in response to *C. rodentium* was significantly decreased in the presence of a Rac1 inhibitor (Figure 6G). Therefore, in *C. rodentium*-challenged macrophages, Rac1 appears to link β2-integrins to ROS production, in turn suggesting that Rac1 may also regulate IL-1β. Rac1 inhibition with NSC23766 significantly decreased IL-1β secretion in *C. rodentium*-challenged CD18$^{+/-}$ BMDMs and in intestinal F4/80^{+}CX3CR1^{+} macrophages, and further diminished IL-1β levels in similarly challenged CD18$^{-/-}$ cells (Figures 6H and S6A). These data indicate that Rac1 functions downstream of β2-integrin and promotes ROS generation. It is likely that CD18$^{-/-}$ macrophages have additional defects, such as impaired opsonophagocytosis of *C. rodentium*, a notion that we confirmed (Figure S6C). However, CD11b$^{-/-}$ mice, which lack complement receptor 3 (CD11b/CD18) that mediates complement-dependent opsonophagocytosis, do not exhibit lethal *C. rodentium*-induced colitis as seen in CD18$^{-/-}$ mice (data not shown).

Our data collectively indicate that β2-integrins promote IL-1β production in macrophages via Rac1-dependent ROS production, which in turn regulates caspase-11. These mechanistic findings, in combination with the IL-1β requirement for efficient IL-22 production in macrophage-ILC3 co-cultures (Figure 5F), are consistent with our *in vivo* observations for defective production of IL-1β, and hence IL-22, in the colon of *C. rodentium*-infected CD18$^{-/-}$ mice.

DISCUSSION

Our study shows that β2-integrins are required for optimal IL-22 responses by intestinal ILC3s and protection from *C. rodentium*-induced colitis. Mechanistically, β2-integrin deficiency did not affect ILC3s in a cell-intrinsic manner, but through defective production of paracrine IL-1β, a macrophage-derived cytokine that promotes IL-22 production by ILC3s (Longman et al., 2014; Seo et al., 2015). Our findings thus reveal a connection between β2-integrins and Rac1-dependent, ROS-mediated activation of the noncanonical NLRP3 inflammasome-IL-1β axis. Given the importance of IL-22 in intestinal homeostasis and immunity (Cella et al., 2009; Zenewicz et al., 2008; Zheng et al., 2008), the functional link between β2-integrins and IL-22 provides a mechanistic understanding of the marked susceptibility of

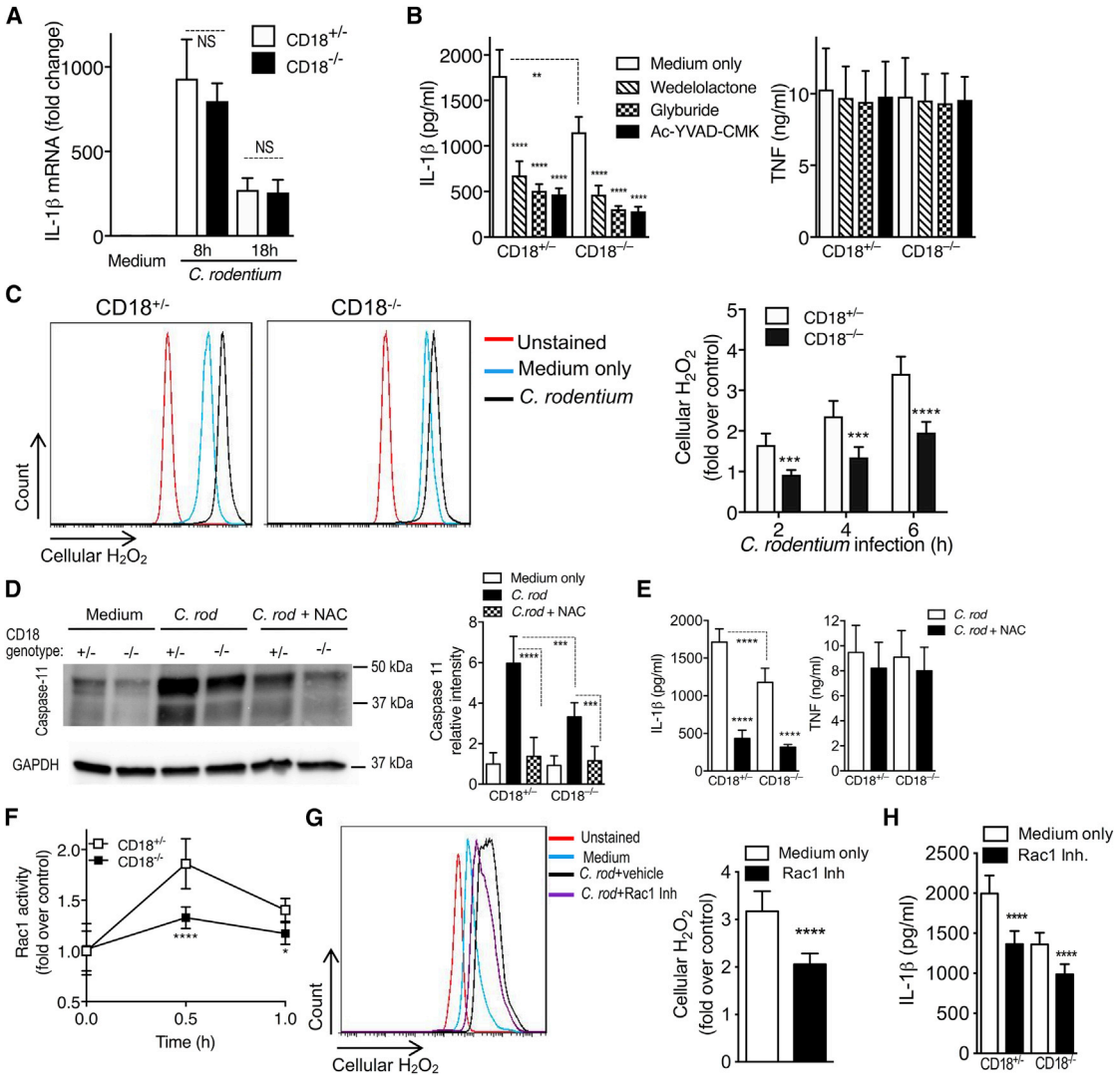

Figure 6. β2-Integrins Promote Rac1-Dependent ROS Production and Noncanonical Inflammasome Activation

(A) CD18$^{+/-}$ and CD18$^{-/-}$ BMDMs were infected with *C. rodentium* at an MOI of 20:1, and IL-1β mRNA expression was determined at 8 and 18 h post-infection by quantitative real-time PCR.

(B) CD18$^{+/-}$ and CD18$^{-/-}$ BMDMs were pre-treated for 1 h with the indicated inhibitors and then infected with *C. rodentium* for 18 h. Supernatants were harvested and analyzed for IL-1β and TNF release by ELISA.

(C) CD18$^{+/-}$ and CD18$^{-/-}$ BMDMs were stimulated with *C. rodentium* (MOI = 20:1), stained with H2DCFDA, and analyzed by flow cytometry; shown are representative FACS plots (left) and data analysis (fold increase over unstimulated control) at the indicated times (right).

(D and E) CD18$^{+/-}$ and CD18$^{-/-}$ BMDMs were pre-treated with 20 mM NAC for 1 h and then infected with *C. rodentium* (MOI = 20:1).

(D) At 16 h post infection, cell lysates were harvested and analyzed by immunoblotting with anti-mouse-caspase-11 antibody (left) and densitometry (right).

(E) At 18 h post infection, supernatants were harvested and analyzed for IL-1β and TNF release by ELISA.

(F) CD18$^{+/-}$ and CD18$^{-/-}$ BMDMs were stimulated with *C. rodentium* (MOI = 20:1), and Rac1 activity was determined using the Rac1 G-LISA activation assay and expressed as fold increase over unstimulated control.

(G and H) CD18$^{+/-}$ and CD18$^{-/-}$ BMDMs were pre-treated with Rac1 inhibitor (NSC23766; 100 μM) for 1 h and then infected with *C. rodentium* (MOI = 20:1).

(G) At 6 h post-infection, cells were stained with H2DCFDA and analyzed by flow cytometry; shown are representative FACS plots (left) and data analysis (right).

(H) At 18 h post-infection, supernatants were harvested and analyzed for IL-1β release by ELISA.

Data are means ± SDs and are pooled from 2 independent experiments performed in triplicate for a total of 6 replicates/group (A–C); are from 3 independent experiments with 2 or 3 replicates/group for a total of 6–7 replicates/group (D); are from 3 independent experiments performed in triplicate in 2 experiments and in duplicate in 1 experiment, for a total of 8 replicates/group (E); or are from 3 independent experiments performed in triplicate, for a total of 9 replicates/group (F–H). *$p < 0.05$, **$p < 0.01$, ***$p < 0.001$, and ****$p < 0.0001$ (B: 1-way ANOVA with Dunnett's multiple comparisons test; F: 2-way ANOVA with Sidak's multiple comparisons test; A, C–E, G, and H: 2-tailed Student's t test). NS, non-significant.

LAD1 ($CD18^{-/-}$) mice to colitis, which was reversed by exogenous administration of IL-22-Fc.

Caspase-11 functions both as a sensor of Gram-negative bacterial infections, such as by *C. rodentium*, and as a trigger of NLRP3 inflammasome assembly in the noncanonical pathway, thus acting upstream of caspase-1 (Kayagaki et al., 2013; Sharma and Kanneganti, 2016). In *C. rodentium*-challenged macrophages, induction of ROS upregulates caspase-11 expression and promotes noncanonical NLRP3 inflammasome activation (Lupfer et al., 2014). Here, we found that *C. rodentium*-challenged macrophages are defective in Rac1 activation and hence in ROS production in the absence of β2-integrin expression. The ability of β2-integrins to upregulate ROS production renders them an important regulator of noncanonical NLRP3 inflammasome-dependent release of IL-1β. Although *C. rodentium*-challenged $CD18^{-/-}$ macrophages exhibited impaired IL-1β release, they expressed normal levels of IL-1β mRNA and elicited TNF and IL-6 protein responses similar to those of CD18-sufficient macrophages, suggesting a selective defect of β2-integrin deficiency in inflammasome activation. It should be noted that IL-1β production is not the only defect expected in $CD18^{-/-}$ macrophages, and in this regard, other β2-integrin-dependent functions in macrophages include phagocytosis of microbes opsonized with C3 activation fragments, adhesion to extracellular matrix components such as fibrinogen, and podosome formation (Erdei et al., 2019). Although $CD18^{-/-}$ macrophages display impaired *C. rodentium* opsonophagocytosis *in vitro*, which may contribute to the $CD18^{-/-}$ phenotype in the *C. rodentium* infection model, $CD11b^{-/-}$ mice do not develop lethal *C. rodentium*-induced colitis as $CD18^{-/-}$ mice do. Thus, defective phagocytosis may not necessarily be a crucial defect in this regard, although complement receptor 4 (CD11c/CD18) may compensate for the lack of complement receptor 3 (CD11b/CD18) in $CD11b^{-/-}$ mice.

Our findings that the colons of *C. rodentium*-infected $CD18^{-/-}$ mice and CD18-sufficient ($CD18^{+/-}$) controls contain comparable numbers of $F4/80^{+}CX3CR1^{+}$ macrophages lend further support to the concept that the reduced production of colonic IL-1β in $CD18^{-/-}$ mice arises from cell-intrinsic defects in the macrophages (owing to their CD18 deficiency), as it cannot be attributed to the reduced abundance of macrophages in these mice. That $CD18^{-/-}$ monocytes or macrophages may exhibit normal transmigration in some cases is consistent with observations that other integrins, such as very late antigen-4 (VLA-4), can also mediate macrophage accumulation in an inflamed tissue (Chung et al., 2017; Meerschaert and Furie, 1995). Whereas CD18 has been implicated in multiple pathologies predominantly as a recruitment receptor (Palmen et al., 1995; Suchard et al., 2010; Vedder et al., 1988; Wallace et al., 1992), our study has clearly distinguished the recruitment function of CD18 from its immune activation function in intestinal macrophages.

An earlier study investigated $CD18^{-/-}$ mice in dextran sodium sulfate (DSS)-induced colitis and found that they were less susceptible to DSS than were wild-type mice (Abdelbaqi et al., 2006). As DSS-induced colitis is largely due to excessive neutrophil recruitment, the authors attributed the protective effect of CD18 deficiency to the diminished numbers of recruited neutrophils in the intestines of the $CD18^{-/-}$ mice. Because the model we used is driven by infection, and thus host immunity plays a central role, the importance of CD18 for maximal activation of the ROS-noncanonical NLRP3-IL-1β pathway has led to the pronounced susceptibility of the $CD18^{-/-}$ mice, as compared to their wild-type littermate controls. The use of different models (likely addressing distinct functions of CD18) may explain the seemingly disparate results in the two studies.

$IL\text{-}22^{-/-}$ mice (Zheng et al., 2008) and $CD18^{-/-}$ mice (the present study) succumb within the second week after inoculation of *C. rodentium* ("early stage of infection"), whereas mice lacking adaptive immunity (recombinase activating gene-1-deficient [$Rag1^{-/-}$] mice) start dying after the second week of infection (Vallance et al., 2002). ILC3s constitute the dominant source of IL-22 in the early stage of *C. rodentium* infection (Cella et al., 2009; Seo et al., 2015; Sonnenberg et al., 2011; Zheng et al., 2008), whereas at later time points, IL-22-producing $CD4^{+}$ T cells assume a leading role in protection against *C. rodentium*-induced colitis (Basu et al., 2012). Consistent with these findings, all of the *C. rodentium*-infected $IL\text{-}22^{-/-}$ mice administered $IL\text{-}22^{+/+}$ $CD4^{+}$ T cells succumbed to infection within the second week, whereas 50% of $IL\text{-}22^{-/-}$ mice given $IL\text{-}22^{+/+}$ ILC3s survived beyond day 20 (Sonnenberg et al., 2011). In line with these studies, IL-22-producing T cells were not detectable in the colons of *C. rodentium*-infected $CD18^{-/-}$ mice or their CD18-sufficient ($CD18^{+/-}$) littermate controls at day 8 post-infection. Therefore, the IL-22 defect underlying the pronounced susceptibility of $CD18^{-/-}$ mice to *C. rodentium* infection involves ILC3s and not other potential cellular sources of this cytokine, such as CD4 T cells. Overall, ILC3-derived IL-22 is critical for intestinal innate immunity to *C. rodentium* infection before adaptive immunity can fully develop.

Consistent with the protective function of IL-22 in mouse models of colitis (Sugimoto et al., 2008; Zenewicz et al., 2008), the secreted IL-22-binding protein (IL-22BP) exacerbates experimental colitis by blocking the binding of IL-22 to its receptor (Pelczar et al., 2016). In humans with inflammatory bowel disease (IBD), anti-TNF therapy inhibited the expression of IL-22BP in patients who responded to therapy, suggesting a protective role for IL-22 in human colitis (Pelczar et al., 2016), perhaps through its ability to induce antimicrobial molecules and mucus production and to promote mucosal healing and barrier integrity (Hernandez et al., 2018; Sabat et al., 2014). Consistent with these findings, IL-22-related molecules (e.g., IL-10R2 and signal transducer and activator of transcription 3 [STAT3]) are encoded by inflammatory bowel disease susceptibility genes (Glocker et al., 2009; Silverberg et al., 2009). Moreover, the frequency of IL-22-secreting ILCs in the intestinal lamina propria is markedly decreased in patients with Crohn disease (Takayama et al., 2010). However, the exact role of IL-22 in colitis requires further investigation (Sabat et al., 2014). Whereas colitis in an LAD1 patient was completely resolved after bone marrow transplantation (D'Agata et al., 1996), patients for whom transplantation is not an option may benefit from therapies that promote intestinal immunity and homeostasis.

We have recently shown that the association of LAD1 with the oral inflammatory disease periodontitis is driven by microbe-induced hyperinflammatory responses involving the

IL-23-IL-17 immune pathway (Moutsopoulos et al., 2014). Accordingly, antibody-mediated inhibition of IL-23 or IL-17 diminished inflammation and bone loss in a mouse model of LAD1 periodontitis (Moutsopoulos et al., 2014). Moreover, systemic administration of ustekinumab (which targets the common p40 subunit of IL-23 and IL-12) in a human LAD1 patient resulted in the inhibition of IL-17 expression, resolution of inflammatory periodontal lesions, and healing of a severe sacral wound that also featured abundant IL-17 expression (Moutsopoulos et al., 2017). Although CD18$^{-/-}$ mice displayed dysregulated overexpression of IL-17 in the gut upon *C. rodentium* challenge, neutralization of this cytokine failed to change the disease course and to increase IL-22 production, suggesting that the IL-23-IL-17 axis may drive the pathogenesis of some (e.g., periodontal lesions, skin lesions) but not all conditions associated with LAD1.

We found that, unlike CD18$^{-/-}$ mice, CXCR2$^{-/-}$ mice survive infection with *C. rodentium* despite tissue inflammation and reduced bacterial clearance, and these findings are consistent with an earlier report (Spehlmann et al., 2009). That study showed that the defective recruitment of neutrophils to the colon of CXCR2$^{-/-}$ mice results in increased tissue pathology and bacterial load (as compared to wild-type controls) in the colons, livers, and spleens at the "early stage of infection," specifically 2 weeks post-infection. However, the same study showed that *C. rodentium*-infected CXCR2$^{-/-}$ mice did not die and eventually cleared the bacteria after 4 weeks (Spehlmann et al., 2009). In contrast, neutrophil-deficient LysM^{cre}Mcl1$^{fl/fl}$ mice succumb to *C. rodentium* infection by day 14 (Kamada et al., 2015). However, the defect in these mice does not simply involve the scarcity of neutrophils from peripheral tissues such as the colon, but neutrophils are globally absent (including from the circulation, where both CXCR2$^{-/-}$and CD18$^{-/-}$ mice exhibit neutrophilia [Mei et al., 2012; Scharffetter-Kochanek et al., 1998; Stark et al., 2005]). Thus, mortality in the LysM^{cre}Mcl1$^{fl/fl}$ mouse model may, at least in part, result from systemic dissemination of bacteria to vital organs in the absence of systemic neutrophil defense. These findings collectively suggest that the protection conferred by β2 integrins in the early stage of *C. rodentium* infection is unlikely to be primarily attributed to their capacity to mediate neutrophil recruitment; rather, it may be associated with the induction of Rac1- and ROS-mediated noncanonical NLRP3 inflammasome-dependent IL-1β production. This in turn promotes ILC3-derived IL-22 production and protection against lethal *C. rodentium*-induced colitis, as shown in the present study.

The association of β2-integrins with inflammatory diseases, including colitis, often involves their ability to mediate pathologic infiltration of inflammatory leukocytes to infected or inflamed tissues (Kourtzelis et al., 2017; Palmen et al., 1995; Rothhammer et al., 2011; Suchard et al., 2010; Vedder et al., 1988; Wallace et al., 1992). Here, in contrast, we established a protective function for β2-integrins in promoting IL-1β-dependent IL-22 responses that inhibit *C. rodentium*-induced colitis. Our study therefore suggests a plausible link between LAD1 and susceptibility to colitogenic bacteria. Our findings that β2-integrins promote intestinal immunity should be considered in the context of β2-integrin targeting strategies to control the leukocyte adhesion cascade as a potential therapy in inflammatory bowel disease (Bamias et al., 2013).

STAR★METHODS

Detailed methods are provided in the online version of this paper and include the following:

- KEY RESOURCES TABLE
- CONTACT FOR REAGENT AND RESOURCE SHARING
- EXPERIMENTAL MODEL AND SUBJECT DETAILS
  - Mice
- METHOD DETAILS
  - C. rodentium infection and *in vivo* treatments
  - Fluorescence *in situ* hybridization (FISH)
  - Histology
  - Cell isolation and flow cytometry
  - Quantitative real-time PCR
  - ELISA of *ex vivo* cytokine responses
  - *In vitro* stimulation of macrophages and ILC3s
  - ROS measurement
  - Rac1 activation assay
  - Opsonophagocytosis
- QUANTIFICATION AND STATISTICAL ANALYSIS
  - Statistical analysis

SUPPLEMENTAL INFORMATION

Supplemental Information includes six figures and can be found with this article online at https://doi.org/10.1016/j.celrep.2019.01.054.

ACKNOWLEDGMENTS

This work was supported by grants from the NIH (DE024153, DE024716, DE015254, and AI068730 to G.H. and DE026152 to G.H. and T.C.), the Intramural Research Program of the National Institute for Dental and Craniofacial Research (NIDCR) (to N.M.M.), the Deutsche Forschungsgemeinschaft (SFB-TR 205 to T.C.), the European Research Council (ERC) (DEMETINL to T.C.), and the Rabinowitz Research Award (to B.W.). B.A.V. is the Children with Intestinal and Liver Disorders (Ch.I.L.D.) Foundation Research Chair in Pediatric Gastroenterology.

AUTHOR CONTRIBUTIONS

B.W. designed the study, performed experiments, analyzed and interpreted the data, and wrote the manuscript; J.-H.L., T.K., and X.L. performed experiments and analyzed and interpreted the data; B.A.V. generated critical reagents and edited the paper; N.M.M. interpreted the data and edited the paper; T.C. designed experiments, interpreted the data, and edited the paper; and G.H. conceived and designed the study, supervised the research, interpreted the data, and wrote the manuscript.

DECLARATION OF INTERESTS

The authors declare no competing interests.

Received: September 5, 2018
Revised: December 7, 2018
Accepted: January 15, 2019
Published: February 5, 2019

REFERENCES

Abdelbaqi, M., Chidlow, J.H., Matthews, K.M., Pavlick, K.P., Barlow, S.C., Linscott, A.J., Grisham, M.B., Fowler, M.R., and Kevil, C.G. (2006). Regulation of

dextran sodium sulfate induced colitis by leukocyte beta 2 integrins. Lab. Invest. *86*, 380–390.

Bamias, G., Clark, D.J., and Rivera-Nieves, J. (2013). Leukocyte traffic blockade as a therapeutic strategy in inflammatory bowel disease. Curr. Drug Targets *14*, 1490–1500.

Basu, R., O'Quinn, D.B., Silberger, D.J., Schoeb, T.R., Fouser, L., Ouyang, W., Hatton, R.D., and Weaver, C.T. (2012). Th22 cells are an important source of IL-22 for host protection against enteropathogenic bacteria. Immunity *37*, 1061–1075.

Bergstrom, K.S., Kissoon-Singh, V., Gibson, D.L., Ma, C., Montero, M., Sham, H.P., Ryz, N., Huang, T., Velcich, A., Finlay, B.B., et al. (2010). Muc2 protects against lethal infectious colitis by disassociating pathogenic and commensal bacteria from the colonic mucosa. PLoS Pathog. *6*, e1000902.

Broz, P., and Monack, D.M. (2013). Measuring inflammasome activation in response to bacterial infection. Methods Mol. Biol. *1040*, 65–84.

Caballero, S., Carter, R., Ke, X., Sušac, B., Leiner, I.M., Kim, G.J., Miller, L., Ling, L., Manova, K., and Pamer, E.G. (2015). Distinct but Spatially Overlapping Intestinal Niches for Vancomycin-Resistant Enterococcus faecium and Carbapenem-Resistant Klebsiella pneumoniae. PLoS Pathog. *11*, e1005132.

Cella, M., Fuchs, A., Vermi, W., Facchetti, F., Otero, K., Lennerz, J.K., Doherty, J.M., Mills, J.C., and Colonna, M. (2009). A human natural killer cell subset provides an innate source of IL-22 for mucosal immunity. Nature *457*, 722–725.

Chung, K.J., Chatzigeorgiou, A., Economopoulou, M., Garcia-Martin, R., Alexaki, V.I., Mitroulis, I., Nati, M., Gebler, J., Ziemssen, T., Goelz, S.E., et al. (2017). A self-sustained loop of inflammation-driven inhibition of beige adipogenesis in obesity. Nat. Immunol. *18*, 654–664.

D'Agata, I.D., Paradis, K., Chad, Z., Bonny, Y., and Seidman, E. (1996). Leucocyte adhesion deficiency presenting as a chronic ileocolitis. Gut *39*, 605–608.

Erdei, A., Lukacsi, S., Macsik-Valent, B., Nagy-Balo, Z., Kurucz, I., and Bajtay, Z. (2019). Non-identical twins: different faces of CR3 and CR4 in myeloid and lymphoid cells of mice and men. Semin. Cell Dev. Biol. *85*, 110–121.

Giacomin, P.R., Moy, R.H., Noti, M., Osborne, L.C., Siracusa, M.C., Alenghat, T., Liu, B., McCorkell, K.A., Troy, A.E., Rak, G.D., et al. (2015). Epithelial-intrinsic IKKα expression regulates group 3 innate lymphoid cell responses and antibacterial immunity. J. Exp. Med. *212*, 1513–1528.

Glocker, E.O., Kotlarz, D., Boztug, K., Gertz, E.M., Schäffer, A.A., Noyan, F., Perro, M., Diestelhorst, J., Allroth, A., Murugan, D., et al. (2009). Inflammatory bowel disease and mutations affecting the interleukin-10 receptor. N. Engl. J. Med. *361*, 2033–2045.

Hanna, S., and Etzioni, A. (2012). Leukocyte adhesion deficiencies. Ann. N Y Acad. Sci. *1250*, 50–55.

Hawkins, H.K., Heffelfinger, S.C., and Anderson, D.C. (1992). Leukocyte adhesion deficiency: clinical and postmortem observations. Pediatr. Pathol. *12*, 119–130.

Heasman, S.J., and Ridley, A.J. (2008). Mammalian Rho GTPases: new insights into their functions from in vivo studies. Nat. Rev. Mol. Cell Biol. *9*, 690–701.

Hepworth, M.R., Fung, T.C., Masur, S.H., Kelsen, J.R., McConnell, F.M., Dubrot, J., Withers, D.R., Hugues, S., Farrar, M.A., Reith, W., et al. (2015). Immune tolerance. Group 3 innate lymphoid cells mediate intestinal selection of commensal bacteria-specific $CD4^+$ T cells. Science *348*, 1031–1035.

Hernandez, P., Gronke, K., and Diefenbach, A. (2018). A catch-22: interleukin-22 and cancer. Eur. J. Immunol. *48*, 15–31.

Kamada, N., Sakamoto, K., Seo, S.U., Zeng, M.Y., Kim, Y.G., Cascalho, M., Vallance, B.A., Puente, J.L., and Núñez, G. (2015). Humoral Immunity in the Gut Selectively Targets Phenotypically Virulent Attaching-and-Effacing Bacteria for Intraluminal Elimination. Cell Host Microbe *17*, 617–627.

Kayagaki, N., Warming, S., Lamkanfi, M., Vande Walle, L., Louie, S., Dong, J., Newton, K., Qu, Y., Liu, J., Heldens, S., et al. (2011). Non-canonical inflammasome activation targets caspase-11. Nature *479*, 117–121.

Kayagaki, N., Wong, M.T., Stowe, I.B., Ramani, S.R., Gonzalez, L.C., Akashi-Takamura, S., Miyake, K., Zhang, J., Lee, W.P., Muszyński, A., et al. (2013). Noncanonical inflammasome activation by intracellular LPS independent of TLR4. Science *341*, 1246–1249.

Koroleva, E.P., Halperin, S., Gubernatorova, E.O., Macho-Fernandez, E., Spencer, C.M., and Tumanov, A.V. (2015). Citrobacter rodentium-induced colitis: a robust model to study mucosal immune responses in the gut. J. Immunol. Methods *421*, 61–72.

Kourtzelis, I., Mitroulis, I., von Renesse, J., Hajishengallis, G., and Chavakis, T. (2017). From leukocyte recruitment to resolution of inflammation: the cardinal role of integrins. J. Leukoc. Biol. *102*, 677–683.

Lamkanfi, M., and Dixit, V.M. (2014). Mechanisms and functions of inflammasomes. Cell *157*, 1013–1022.

Longman, R.S., Diehl, G.E., Victorio, D.A., Huh, J.R., Galan, C., Miraldi, E.R., Swaminath, A., Bonneau, R., Scherl, E.J., and Littman, D.R. (2014). CX_3CR1^+ mononuclear phagocytes support colitis-associated innate lymphoid cell production of IL-22. J. Exp. Med. *211*, 1571–1583.

Lupfer, C.R., Anand, P.K., Liu, Z., Stokes, K.L., Vogel, P., Lamkanfi, M., and Kanneganti, T.D. (2014). Reactive oxygen species regulate caspase-11 expression and activation of the non-canonical NLRP3 inflammasome during enteric pathogen infection. PLoS Pathog. *10*, e1004410.

Manta, C., Heupel, E., Radulovic, K., Rossini, V., Garbi, N., Riedel, C.U., and Niess, J.H. (2013). CX(3)CR1(+) macrophages support IL-22 production by innate lymphoid cells during infection with Citrobacter rodentium. Mucosal Immunol. *6*, 177–188.

Meerschaert, J., and Furie, M.B. (1995). The adhesion molecules used by monocytes for migration across endothelium include CD11a/CD18, CD11b/CD18, and VLA-4 on monocytes and ICAM-1, VCAM-1, and other ligands on endothelium. J. Immunol. *154*, 4099–4112.

Mei, J., Liu, Y., Dai, N., Hoffmann, C., Hudock, K.M., Zhang, P., Guttentag, S.H., Kolls, J.K., Oliver, P.M., Bushman, F.D., and Worthen, G.S. (2012). Cxcr2 and Cxcl5 regulate the IL-17/G-CSF axis and neutrophil homeostasis in mice. J. Clin. Invest. *122*, 974–986.

Moutsopoulos, N.M., Konkel, J., Sarmadi, M., Eskan, M.A., Wild, T., Dutzan, N., Abusleme, L., Zenobia, C., Hosur, K.B., Abe, T., et al. (2014). Defective neutrophil recruitment in leukocyte adhesion deficiency type I disease causes local IL-17-driven inflammatory bone loss. Sci. Transl. Med. *6*, 229ra40.

Moutsopoulos, N.M., Zerbe, C.S., Wild, T., Dutzan, N., Brenchley, L., DiPasquale, G., Uzel, G., Axelrod, K.C., Lisco, A., Notarangelo, L.D., et al. (2017). Interleukin-12 and Interleukin-23 Blockade in Leukocyte Adhesion Deficiency Type 1. N. Engl. J. Med. *376*, 1141–1146.

Nurmi, S.M., Autero, M., Raunio, A.K., Gahmberg, C.G., and Fagerholm, S.C. (2007). Phosphorylation of the LFA-1 integrin beta2-chain on Thr-758 leads to adhesion, Rac-1/Cdc42 activation, and stimulation of CD69 expression in human T cells. J. Biol. Chem. *282*, 968–975.

Ota, N., Wong, K., Valdez, P.A., Zheng, Y., Crellin, N.K., Diehl, L., and Ouyang, W. (2011). IL-22 bridges the lymphotoxin pathway with the maintenance of colonic lymphoid structures during infection with Citrobacter rodentium. Nat. Immunol. *12*, 941–948.

Palmen, M.J., Dijkstra, C.D., van der Ende, M.B., Peña, A.S., and van Rees, E.P. (1995). Anti-CD11b/CD18 antibodies reduce inflammation in acute colitis in rats. Clin. Exp. Immunol. *101*, 351–356.

Pelczar, P., Witkowski, M., Perez, L.G., Kempski, J., Hammel, A.G., Brockmann, L., Kleinschmidt, D., Wende, S., Haueis, C., Bedke, T., et al. (2016). A pathogenic role for T cell-derived IL-22BP in inflammatory bowel disease. Science *354*, 358–362.

Rathinam, V.A., Vanaja, S.K., Waggoner, L., Sokolovska, A., Becker, C., Stuart, L.M., Leong, J.M., and Fitzgerald, K.A. (2012). TRIF licenses caspase-11-dependent NLRP3 inflammasome activation by gram-negative bacteria. Cell *150*, 606–619.

Rothhammer, V., Heink, S., Petermann, F., Srivastava, R., Claussen, M.C., Hemmer, B., and Korn, T. (2011). Th17 lymphocytes traffic to the central nervous system independently of α4 integrin expression during EAE. J. Exp. Med. *208*, 2465–2476.

Sabat, R., Ouyang, W., and Wolk, K. (2014). Therapeutic opportunities of the IL-22-IL-22R1 system. Nat. Rev. Drug Discov. *13*, 21–38.

Scharffetter-Kochanek, K., Lu, H., Norman, K., van Nood, N., Munoz, F., Grabbe, S., McArthur, M., Lorenzo, I., Kaplan, S., Ley, K., et al. (1998). Spontaneous skin ulceration and defective T cell function in CD18 null mice. J. Exp. Med. *188*, 119–131.

Schmidt, S., Moser, M., and Sperandio, M. (2013). The molecular basis of leukocyte recruitment and its deficiencies. Mol. Immunol. *55*, 49–58.

Seo, S.U., Kuffa, P., Kitamoto, S., Nagao-Kitamoto, H., Rousseau, J., Kim, Y.G., Núñez, G., and Kamada, N. (2015). Intestinal macrophages arising from CCR2(+) monocytes control pathogen infection by activating innate lymphoid cells. Nat. Commun. *6*, 8010.

Sharma, D., and Kanneganti, T.D. (2016). The cell biology of inflammasomes: mechanisms of inflammasome activation and regulation. J. Cell Biol. *213*, 617–629.

Silverberg, M.S., Cho, J.H., Rioux, J.D., McGovern, D.P., Wu, J., Annese, V., Achkar, J.P., Goyette, P., Scott, R., Xu, W., et al. (2009). Ulcerative colitis-risk loci on chromosomes 1p36 and 12q15 found by genome-wide association study. Nat. Genet. *41*, 216–220.

Sonnenberg, G.F., and Artis, D. (2015). Innate lymphoid cells in the initiation, regulation and resolution of inflammation. Nat. Med. *21*, 698–708.

Sonnenberg, G.F., Nair, M.G., Kirn, T.J., Zaph, C., Fouser, L.A., and Artis, D. (2010). Pathological versus protective functions of IL-22 in airway inflammation are regulated by IL-17A. J. Exp. Med. *207*, 1293–1305.

Sonnenberg, G.F., Monticelli, L.A., Elloso, M.M., Fouser, L.A., and Artis, D. (2011). CD4(+) lymphoid tissue-inducer cells promote innate immunity in the gut. Immunity *34*, 122–134.

Spehlmann, M.E., Dann, S.M., Hruz, P., Hanson, E., McCole, D.F., and Eckmann, L. (2009). CXCR2-dependent mucosal neutrophil influx protects against colitis-associated diarrhea caused by an attaching/effacing lesion-forming bacterial pathogen. J. Immunol. *183*, 3332–3343.

Stark, M.A., Huo, Y., Burcin, T.L., Morris, M.A., Olson, T.S., and Ley, K. (2005). Phagocytosis of apoptotic neutrophils regulates granulopoiesis via IL-23 and IL-17. Immunity *22*, 285–294.

Suchard, S.J., Stetsko, D.K., Davis, P.M., Skala, S., Potin, D., Launay, M., Dhar, T.G., Barrish, J.C., Susulic, V., Shuster, D.J., et al. (2010). An LFA-1 (alphaLbeta2) small-molecule antagonist reduces inflammation and joint destruction in murine models of arthritis. J. Immunol. *184*, 3917–3926.

Sugimoto, K., Ogawa, A., Mizoguchi, E., Shimomura, Y., Andoh, A., Bhan, A.K., Blumberg, R.S., Xavier, R.J., and Mizoguchi, A. (2008). IL-22 ameliorates intestinal inflammation in a mouse model of ulcerative colitis. J. Clin. Invest. *118*, 534–544.

Takayama, T., Kamada, N., Chinen, H., Okamoto, S., Kitazume, M.T., Chang, J., Matuzaki, Y., Suzuki, S., Sugita, A., Koganei, K., et al. (2010). Imbalance of NKp44(+)NKp46(-) and NKp44(-)NKp46(+) natural killer cells in the intestinal mucosa of patients with Crohn's disease. Gastroenterology *139*, 882–892, 892 e1–892e3.

Uzel, G., Kleiner, D.E., Kuhns, D.B., and Holland, S.M. (2001). Dysfunctional LAD-1 neutrophils and colitis. Gastroenterology *121*, 958–964.

Vallance, B.A., Deng, W., Knodler, L.A., and Finlay, B.B. (2002). Mice lacking T and B lymphocytes develop transient colitis and crypt hyperplasia yet suffer impaired bacterial clearance during Citrobacter rodentium infection. Infect. Immun. *70*, 2070–2081.

Vedder, N.B., Winn, R.K., Rice, C.L., Chi, E.Y., Arfors, K.E., and Harlan, J.M. (1988). A monoclonal antibody to the adherence-promoting leukocyte glycoprotein, CD18, reduces organ injury and improves survival from hemorrhagic shock and resuscitation in rabbits. J. Clin. Invest. *81*, 939–944.

Wallace, J.L., Higa, A., McKnight, G.W., and MacIntyre, D.E. (1992). Prevention and reversal of experimental colitis by a monoclonal antibody which inhibits leukocyte adherence. Inflammation *16*, 343–354.

Wang, B., Zhuang, X., Deng, Z.B., Jiang, H., Mu, J., Wang, Q., Xiang, X., Guo, H., Zhang, L., Dryden, G., et al. (2014). Targeted drug delivery to intestinal macrophages by bioactive nanovesicles released from grapefruit. Mol. Ther. *22*, 522–534.

West, A.P., Brodsky, I.E., Rahner, C., Woo, D.K., Erdjument-Bromage, H., Tempst, P., Walsh, M.C., Choi, Y., Shadel, G.S., and Ghosh, S. (2011). TLR signalling augments macrophage bactericidal activity through mitochondrial ROS. Nature *472*, 476–480.

Withers, D.R., Hepworth, M.R., Wang, X., Mackley, E.C., Halford, E.E., Dutton, E.E., Marriott, C.L., Brucklacher-Waldert, V., Veldhoen, M., Kelsen, J., et al. (2016). Transient inhibition of ROR-γt therapeutically limits intestinal inflammation by reducing TH17 cells and preserving group 3 innate lymphoid cells. Nat. Med. *22*, 319–323.

Xiong, H., Keith, J.W., Samilo, D.W., Carter, R.A., Leiner, I.M., and Pamer, E.G. (2016). Innate Lymphocyte/Ly6C(hi) Monocyte Crosstalk Promotes Klebsiella Pneumoniae Clearance. Cell *165*, 679–689.

Zenewicz, L.A., Yancopoulos, G.D., Valenzuela, D.M., Murphy, A.J., Stevens, S., and Flavell, R.A. (2008). Innate and adaptive interleukin-22 protects mice from inflammatory bowel disease. Immunity *29*, 947–957.

Zenobia, C., Luo, X.L., Hashim, A., Abe, T., Jin, L., Chang, Y., Jin, Z.C., Sun, J.X., Hajishengallis, G., Curtis, M.A., and Darveau, R.P. (2013). Commensal bacteria-dependent select expression of CXCL2 contributes to periodontal tissue homeostasis. Cell. Microbiol. *15*, 1419–1426.

Zheng, Y., Valdez, P.A., Danilenko, D.M., Hu, Y., Sa, S.M., Gong, Q., Abbas, A.R., Modrusan, Z., Ghilardi, N., de Sauvage, F.J., and Ouyang, W. (2008). Interleukin-22 mediates early host defense against attaching and effacing bacterial pathogens. Nat. Med. *14*, 282–289.

STAR★METHODS

KEY RESOURCES TABLE

REAGENT or RESOURCE	SOURCE	IDENTIFIER
Antibodies		
Armenian Hamster anti-mouse CD3e (FITC)	BioLegend	Cat# 100306; RRID: AB_312671
Armenian Hamster anti-mouse CD3e (APC/Cy7)	BioLegend	Cat# 100330; RRID: AB_1877170
Rat anti-mouse CD45	BioLegend	Cat# 103130; RRID: AB_893339
Rat anti-mouse CD5	BioLegend	Cat# 100606; RRID: AB_312735
Rat anti-mouse CD90.2	BioLegend	Cat# 105322; RRID: AB_893453
Rat anti-mouse Ly6G	BioLegend	Cat# 127608; RRID: AB_1186099
Syrian hamster anti-mouse KLRG1	BioLegend	Cat# 138426; RRID: AB_2566554
Rat anti-mouse B220 (FITC)	BioLegend	Cat# 103206; RRID: AB_312991
Rat anti-mouse B220 (Brilliant Violet 421)	BioLegend	Cat# 103240; RRID:AB_11203896
Rat anti-mouse CD127	ThermoFisher	Cat# 25-1271-82; RRID: AB_469649
Rat anti-mouse CD25	BioLegend	Cat# 102012; RRID: AB_312861
Mouse anti-mouse NK1.1	BioLegend	Cat# 108732; RRID: AB_2562218
Rat anti-mouse F4/80	BioLegend	Cat# 123108; RRID: AB_893502
Rat anti-mouse Ly-6G/Ly-6C (Gr-1)	BioLegend	Cat# 108406; RRID: AB_313371
Armenian Hamster anti-mouse TCR γ/δ (FITC)	BioLegend	Cat# 118106; RRID: AB_313830
Armenian Hamster anti-mouse TCR γ/δ (APC)	BioLegend	Cat# 118116; RRID: AB_1731813
Rat anti-mouse IL-17	BioLegend	Cat# 506944; RRID: AB_2566153
Rat anti-mouse IFN-γ	ThermoFisher	Cat# 14-7311-81; RRID: AB_468467
Rat anti-mouse IL-22	ThermoFisher	Cat# 12-7221-82; RRID: AB_10597428
Rat anti-mouse RORγt	ThermoFisher	Cat# 17-6988-82; RRID: AB_10609207
Mouse anti-mouse CX3CR1	BioLegend	Cat# 149007 RRID: AB_2564491
Rat anti-mouse Caspase-11	Novus Biologicals	Cat# NB120-10454
Rabbit anti-mouse GAPDH	Cell Signaling Technology	Cat# 8884S
Rabbit anti- GFP	Abcam	Cat# ab6556
Armenian Hamster anti-mouse IL-1β	Leinco Technologies	Cat# I-437
Armenian Hamster IgG isotype control	Leinco Technologies	Cat# I-140
Rat anti-mouse IL-23 p19	ThermoFisher	Cat# 16-7232-81 RRID: AB_842742
Rat IgG1 kappa Isotype Control	ThermoFisher	Cat# 16-4301-81
InVivoMAb mouse IgG2a isotype control	BioXcell	Cat# BE0085; RRID: AB_1107771
InvivoMAb anti-mouse IL-17A	BioXcell	Cat# BE0173; RRID: AB_10950102
*InVivo*mAb mouse IgG1 isotype control	BioXcell	Cat# BE0083; RRID: AB_1107784
Chemicals, Peptides, and Recombinant Proteins		
Chloramphenicol sodium succinate	Acros Organics	Cat# 459530050
Gentamicin	ThermoFisher	Cat# 15750060
Ac-YVAD-cmk	InvivoGen	Cat# inh-yvad
Brefeldin A	Sigma-Aldrich	Cat# B7651
Wedelolactone	Santa Cruz Biotechnology	Cat# sc-200648
Glyburide	Sigma-Aldrich	Cat# G2539
NSC 23766	Selleckchem	Cat# S8031
N-Acetyl-L-cysteine	Sigma-Aldrich	Cat# A9165
Hydrogen peroxide	MilliporeSigma	Cat# 107209

(*Continued on next page*)

Continued

REAGENT or RESOURCE	SOURCE	IDENTIFIER
H2DCFDA	ThermoFisher	Cat# D399
Collagenase type IV	Worthington Biochemical Corporation	Cat# LS004188
Collagenase type VIII	Sigma-Aldrich	Cat# C2139
DNase I	Sigma-Aldrich	Cat# 10104159001
Ionomycin	Sigma-Aldrich	Cat# I0634
Phorbol 12-myristate 13-acetate	Sigma-Aldrich	Cat# P8139
Protease Inhibitor Cocktail	ThermoFisher	Cat# 87785
IL-22-Fc	Genentech	PRO312045
Recombinant Murine IL-1β	Biolegend	Cat# 575106
Recombinant Murine IL-23	Biolegend	Cat# 589004
Recombinant Murine M-CSF	Biolegend	Cat# 576408
Recombinant Murine IL-7	Biolegend	Cat# 577806
Recombinant Murine IL-15	Biolegend	Cat# 566302
Critical Commercial Assays		
Foxp3/Transcription Factor Buffer Set	ThermoFisher	Cat# 00-5523-00
Mouse G-CSF ELISA	RayBiotech	Cat# ELM-GCSF
Mouse IL-17A ELISA	ThermoFisher	Cat# 88-7371-22
Mouse IL-22 ELISA	ThermoFisher	Cat# 88-7422-22
Mouse IL-1β ELISA	ThermoFisher	Cat# 88-7013-22
Mouse IL-23 ELISA	ThermoFisher	Cat# 88-7230-22
Mouse TNF alpha ELISA	ThermoFisher	Cat# 88-7324-22
Mouse IL-6 ELISA	ThermoFisher	Cat# 88-7064-22
Rac1 G-LISA Activation Assay Kit	Cytoskeleton	Cat# BK128
Trizol	ThermoFisher	Cat# 15596018
High-Capacity RNA-to-cDNA Kit	ThermoFisher	Cat# 4387406
TaqMan Fast Advanced Master Mix	ThermoFisher	Cat# 4444964
Experimental Models: Organisms/Strains		
Mouse: *CD18*$^{-/-}$	The Jackson Laboratory	Stock# 002128
Mouse: *CXCR2*$^{-/-}$	The Jackson Laboratory	Stock# 006848
Mouse: *TCRδ*$^{-/-}$	The Jackson Laboratory	Stock# 002120
Bacterial and Virus Strains		
Citrobacter rodentium strain DBS100	ATCC	Stock# 51459
GFP-expressing and chloramphenicol-resistant *Citrobacter rodentium*	Bergstrom et al., 2010	N/A
Oligonucleotides		
Taqman mouse gene expression assay for *IL-17a*	ThermoFisher	Mm00439619_m1
Taqman mouse gene expression assay for *IL-22*	ThermoFisher	Mm01226722_g1
Taqman mouse gene expression assay for *TNF*	ThermoFisher	Mm00443258_m1
Taqman mouse gene expression assay for *IL-6*	ThermoFisher	Mm00446190_m1
Taqman mouse gene expression assay for *Reg3β*	ThermoFisher	Mm00440616_g1
Taqman mouse gene expression assay for *Reg3γ*	ThermoFisher	Mm00441127_m1
Taqman mouse gene expression assay for *IL-1β*	ThermoFisher	Mm00434228_m1

(*Continued on next page*)

Continued		
REAGENT or RESOURCE	SOURCE	IDENTIFIER
Taqman mouse gene expression assay for *Gapdh*	ThermoFisher	Mm99999915_g1
Universal bacterial probe EUB338 GCTGCCTCCCGTAGGAGT	Bergstrom et al., 2010	N/A
Software and Algorithms		
GraphPad Prism 7	Graphpad Software	V7.0c
QuantStudio Design and Analysis Software	ThermoFisher	V1.4.3
FlowJo version 10	Tree Star	https://www.flowjo.com/solutions/flowjo
AlphaView SA	ProteinSimple	https://www.proteinsimple.com/software_alphaview.html
NIS-Elements AR	Nikon	https://www.microscope.healthcare.nikon.com/products/software/nis-elements/nis-elements-advanced-research

CONTACT FOR REAGENT AND RESOURCE SHARING

Further information and requests for resources and reagents should be directed to and will be fulfilled by the Lead Contact, G. Hajishengallis (geoh@upenn.edu).

EXPERIMENTAL MODEL AND SUBJECT DETAILS

Mice

Mice genetically deficient in all β2 integrins (*CD18*$^{-/-}$), CXCR2 (*CXCR2*$^{-/-}$), or in γδTCR (*Tcrδ*$^{-/-}$) were purchased from the Jackson Laboratories. These mice were crossed with wild-type C57BL/6J mice (Jackson Laboratories) to generate gene-deficient (homozygotes and heterozygotes) mice and wild-type littermate controls for use in experiments. Mice deficient in both CD18 and γδTCR (CD18$^{-/-}$/γδT$^{-/-}$) were generated by breeding the two parental knockout mouse strains. Groups of mice within the same experiment were sex- and age-matched. Male or female mice were used in infection experiments with *C. rodentium* at the age of 8 weeks. As there were no significant differences in the results obtained with males and females (*e.g.*, CD18 deficiency resulted in similar susceptibility to infection regardless of sex), their respective data were pooled. All animal procedures were performed according to protocols reviewed and approved by the Institutional Animal Care and Use Committee of the University of Pennsylvania.

METHOD DETAILS

C. rodentium infection and *in vivo* treatments

Mice were orally gavaged with either 5 × 10^8 colony-forming units (CFU) of *C. rodentium* strain DBS100 (ATCC 51459; American Type Culture Collection) or GFP-expressing and chloramphenicol-resistant *C. rodentium* (GFP-*C. rodentium*) as described (Bergstrom et al., 2010; Zheng et al., 2008). To determine bacterial CFU in the stool, feces were collected, weighed, and homogenized in 5 mL of phosphate-buffered saline (PBS). To enumerate bacterial CFU in MLN, liver and spleen, each organ was homogenized in 2 mL of PBS. Serial dilutions of tissue homogenates were plated onto MacConkey agar (Acumedia; Neogen) or LB agar plate containing chloramphenicol (30μg/ml) and incubated for 24h at 37°C. *C. rodentium* colonies were identified by their characteristic pink center surrounded by a white rim. For *in vivo* neutralization of IL-17, anti-IL-17 monoclonal antibody (200 μg, clone 17F3; BioXcell) and an equal amount of isotype control IgG (IgG1, clone MOPC-21; BioXcell) were administered *i.v.* on a daily basis for 7 days starting 1 day before infection, as previously established (Xiong et al., 2016). To confirm the biological activity of anti-IL-17, blood was obtained by retro-orbital bleeding of CD18$^{-/-}$ and CD18$^{+/-}$ littermates on day 0 and day 4 post-*C. rodentium* infection and the levels of G-CSF in the serum were measured using an ELISA kit (RayBiotech, Inc.). For treatment with IL-22, the mice were *i.v.* injected with 100 μg recombinant IL-22-Fc (IL-22-mIgG2a fusion protein, PRO312045; kindly provided by Genentech) or an equal amount of control IgG (mIgG2a, clone C1.18.4; BioXcell) every three days starting at the day of bacteria inoculation, as previously established (Ota et al., 2011).

Fluorescence *in situ* hybridization (FISH)

Colons from GFP-*C. rodentium*-infected mice were excised and fixed overnight at 4°C in freshly made non-aqueous methacarn solution as previously described (Caballero et al., 2015). Tissues were washed in 70% ethanol, processed with tissue embedding system (KD-BMII) and paraffin-embedded by standard techniques. Sections at 5-μm thickness were baked at 56°C for 1 h prior

to staining. Briefly, tissue sections were deparaffinized with xylene and rehydrated through an ethanol gradient to water. Sections were then incubated at 45°C for 2.5 h with a universal bacterial probe EUB338 (Cy3-GCTGCCTCCCGTAGGAGT-Cy3) directed against the 16S rRNA gene. Subsequently, tissue sections were washed twice and stained with anti-GFP antibody (Abcam) overnight at 4°C. Finally, the sections were further rinsed and counterstained with DAPI (Abcam) and images were captured on a Nikon C2 confocal microscope.

Histology

Large intestines were fixed in 4% paraformaldehyde and then embedded in paraffin. Tissue samples were sectioned at 5-μm thickness and stained with hematoxylin and eosin (H&E) or alcian blue. For histological scoring, tissue sections were blindly graded on a 0-5 scale for each of three parameters (epithelial lesions; inflammation; and edema, hence with an overall maximal histopathology score of 15) as previously described (Giacomin et al., 2015).

Cell isolation and flow cytometry

Spleen and MLNs were harvested and single-cell suspensions were prepared at necropsy (Sonnenberg et al., 2011). Lamina propria mononuclear cells (LPMCs) from intestine were isolated as previously described (Hepworth et al., 2015; Wang et al., 2014). Briefly, intestines were isolated, attached fat was removed and luminal contents were flushed out using PBS. Tissues were cut into 4-cm fragments, everted, gently scraped at the edge of the Petri dish to remove mucus and then rinsed in cold PBS three times. Intraepithelial lymphocytes and epithelial cells were removed by shaking tissue in RPMI-1640 containing penicillin/streptomycin, 0.02 mol/L HEPES, 2% FBS and 2mM EDTA for 30 min at 37°C. LPMCs were isolated by digesting the remaining tissue in 1 mg/ml collagenase type IV (Worthington Biomedical), 1 mg/ml collagenase type VIII and 20 μg/ml DNase I (both from Sigma-Aldrich-Aldrich) for 30min at 37°C. For flow cytometric analysis, cells were stained with monoclonal antibodies (mAbs) against the following surface markers (mAb clone in parenthesis): CD3e (145-2C11), CD5 (53-7.3), CD90.2 (30-H12), Ly6G (1A8), KLRG1 (2F1), B220 (RA3-6B2), CD127 (A7R34), CD25 (PC61), CD45(30-F11), NK1.1 (PK136), F4/80 (BM8), Gr-1(RB6-8C5), RORγt (AFKJS-9), CX3CR1 (SA011F11) and γδT (GL3). All mAbs were purchased from Biolegend. For intracellular detection of cytokines in T cells, the cells were stimulated for 4h with phorbol myristate acetate (50 ng/ml) and ionomycin (750 ng/ml) in the presence of 10 μg/ml brefeldin A (all from Sigma-Aldrich-Aldrich). For intracellular detection of cytokines in ILC3s, cells were first cultured in the presence of mouse recombinant IL-1β and IL-23 each at a concentration of 20 ng/ml for 2h (Biolegend) and then stimulated with phorbol myristate acetate, ionomycin and brefeldin A for 4h, as previously described (Withers et al., 2016). The cells were then fixed and permeabilized using an intracellular fixation and permeabilization kit (ThermoFisher) and stained using antibodies against IL-17 (TC11-18H10.1), IFN-γ (XMG1.2) or IL-22 (1H8PWSR). Flow cytometry data were acquired on LSRII or Accuri (BD Biosciences) and analyzed with FlowJo software (Tree Star Inc.).

Quantitative real-time PCR

Total RNA was extracted from cells or organs using Trizol (ThermoFisher) and quantified by spectrometry at 260 and 280 nm. The RNA was reverse-transcribed using the High Capacity RNA-to-cDNA Kit (ThermoFisher) and real-time PCR with cDNA was performed using the Applied Biosystems 7500 Fast Real-Time PCR System according to the manufacturer's protocol (ThermoFisher). Data were analyzed using the comparative (ΔΔCt) method. TaqMan probes, sense primers, and antisense primers for detection and quantification of genes investigated in this paper were purchased from ThermoFisher. GAPDH was included as an internal control. Samples were normalized to GAPDH and displayed as fold induction over wild-type controls unless otherwise stated.

ELISA of *ex vivo* cytokine responses

For analysis of colon cytokine expression, the distal 3 cm of colonic tissue was excised, cleaned off feces and attached adipose tissue, washed three times with PBS containing fungizone-amphotericin B, penicillin and streptomycin (Wang et al., 2014). Colon segments were further cut into 1-mm pieces and cultured in 1 mL of RPMI-1640 medium supplemented with 10% FBS and 1% amphotericin B-penicilin-streptomycin (ThermoFisher) for 24 h at 37°C with 5% CO2. Supernatants were harvested and the concentration of cytokines was determined by ELISA using specific kits (ThermoFisher). Alternatively, the whole colon was removed, cleaned off fecal material and attached adipose tissue and homogenized in PBS supplemented with proteinase inhibitors (ThermoFisher). The homogenates were then immediately assayed for cytokine production using ELISA kits (ThermoFisher).

In vitro stimulation of macrophages and ILC3s

BM-derived macrophages were generated as described previously (Seo et al., 2015) and cultured for 5 days in DMEM containing 20% L929 supernatant and then re-plated into 24-well plates with antibiotic-free DMEM supplemented with 20 ng/ml of M-CSF. BMDMs were infected with *C. rodentium* at MOI 20:1 for 1h followed by additional incubation, as specified below, in the presence of gentamicin (50 μg/ml) to prevent bacterial overgrowth (Seo et al., 2015). At 8h and 18h post-infection, cells were harvested and processed for quantitative real-time PCR as described above. Culture supernatants were harvested at 18h post-infection and cytokines were measured using ELISA kits (ThermoFisher). Cell lysates were collected at 16h post-infection and analyzed by immunoblotting with anti-mouse-caspase-11 antibody (17D9; Novus Biologicals) (Broz and Monack, 2013). Images were captured using a FluorChem M imaging system (ProteinSimple). Densitometry was performed using the AlphaView software and the data were

normalized against GAPDH. In some experiments, BMDMs were pre-treated with various pharmacological inhibitors for 1h at 37°C prior to infection. For inflammasome inhibition, BMDM were treated with the caspase-1 inhibitor Ac-YVAD-CMK (25μM; Invivogen), caspase-11 inhibitor wedelolactone (30 μM; Santa Cruz Biotechnology) or the NLRP3 inhibitor glyburide (200μM; Sigma-Aldrich). To inhibit Rac1 activation or ROS production, BMDMs were treated with the Rac1 inhibitor NSC23766 (100μM; Selleckchem) or the ROS scavenger N-acetyl-L-cysteine (NAC, 20mM; Sigma-Aldrich), respectively. In other experiments, BMDMs were supplied with 50 μM H_2O_2 as a ROS source 6h after infection with *C. rodentium* (Lupfer et al., 2014) and cell lysates were collected 2.5h later to determine caspase-11 expression by immunoblotting, as described above. To assay cytokine production by intestinal macrophages ($CD45^+CD3^-NK1.1^-B220^-Ly6G^-F4/80^+CX3CR1^+$), these cells were sorting-purified from large intestine of *C. rodentium* infected $CD18^{+/-}$ or $CD18^{-/-}$ littermates using a FACS Aria (BD Bioscience). Intestinal macrophages were pre-treated with various pharmacological inhibitors for 1h at 37°C and then stimulated with *C. rodentium* (MOI 20:1) for 24h. Culture supernatants were harvested for cytokine analysis by ELISA. To assay cytokine responses in ILCs ($CD3^-CD5^-B220^-NK1.1^-F4/80^-Gr\text{-}1^-CD90^+CD127^+CD25^+KLRG1^-$), these cells were sort-purified from intestine and MLN of naive $CD18^{+/-}$ or $CD18^{-/-}$ littermates using a FACS Aria (BD Bioscience). Sorted ILCs at 1×10^5/ml were resuspended in DMEM containing 10 ng/ml IL-7 and 10 ng/ml IL-15. ILCs were either incubated in the presence of 20 ng/ml IL-1β and/or 20 ng/ml IL-23, or in medium alone for 72h. In other experiments, sorted ILCs were co-cultured with BMDMs (both cell types atat 2×10^5/ml) with or without *C. rodentium* (MOI 20:1) for 24h in the presence of neutralizing antibody to IL-1β (10 μg/ml; B122, Leinco Technologies) or an equal concentration of isotype control (Armenian Hamster IgG isotype control monoclonal antibody, PIP, Leinco Technologies). Culture supernatants were harvested and the concentration of cytokines was determined by ELISA using specific kits (ThermoFisher).

ROS measurement

BMDM were plated on non-tissue-culture-treated 12-well plates and stimulated with *C. rodentium* (MOI 20:1) in antibiotic-free medium. At 2, 4 or 6h after infection (West et al., 2011), culture medium was removed and, after washing with PBS, the cells were incubated for 10 min at 37°C in PBS containing 10 μM H2DCFDA (to measure total cellular H_2O_2) (ThermoFisher). Subsequently, the cells were removed from the plate, washed and analyzed immediately by flow cytometry. To control for baseline dye fluorescence, samples were left unstimulated but stained according to the above procedure. Mean fluorescence intensity values were calculated by dividing *C. rodentium*-stimulated by unstimulated values.

Rac1 activation assay

BMDMs were plated in 12-well plates and stimulated with *C. rodentium* (MOI 20:1) in antibiotic-free medium. Cell lysates were harvested at different time points (specified in figure legend) and analyzed for Rac1 activity using the Rac1 G-LISA activation assay kit (Cytoskeleton).

Opsonophagocytosis

For opsonization, GFP-*C. rodentium* bacteria in Hanks' balanced salt solution (containing $CaCl_2$ and $MgCl_2$) were incubated with 50% blood serum obtained from C57BL/6 wild-type mice with end-over-end mixing at 37°C for 30 mins followed by washing. BMDMs were then infected with serum-opsonized GFP-*C. rodentium* (MOI 20:1) at 37°C for 30 mins to allow uptake of bacteria. Cells were treated with gentamycin to kill non-phagocytosed bacteria and harvested by trypsinization, stained with anti-mouse F4/80 antibody (clone BM8, Biolegend), and phagocytic activity (% cells positive for GFP-*C. rodentium*) was determined by flow cytometric analysis.

QUANTIFICATION AND STATISTICAL ANALYSIS

Statistical analysis

Comparison of mean values between groups was evaluated by two-tailed unpaired Student's t test, one-way ANOVA or two-way ANOVA, with repeated-measures as appropriate. The latter two tests were followed by a multiple-comparison post-test, as specified in the figure legends. Statistical analysis was performed using Prism 7.0c (GraphPad Software) and significance was set at $p < 0.05$.

Cell Reports, Volume *26*

Supplemental Information

Macrophage β2-Integrins Regulate IL-22 by ILC3s and Protect from Lethal *Citrobacter rodentium*-Induced Colitis

Baomei Wang, Jong-Hyung Lim, Tetsuhiro Kajikawa, Xiaofei Li, Bruce A. Vallance, Niki M. Moutsopoulos, Triantafyllos Chavakis, and George Hajishengallis

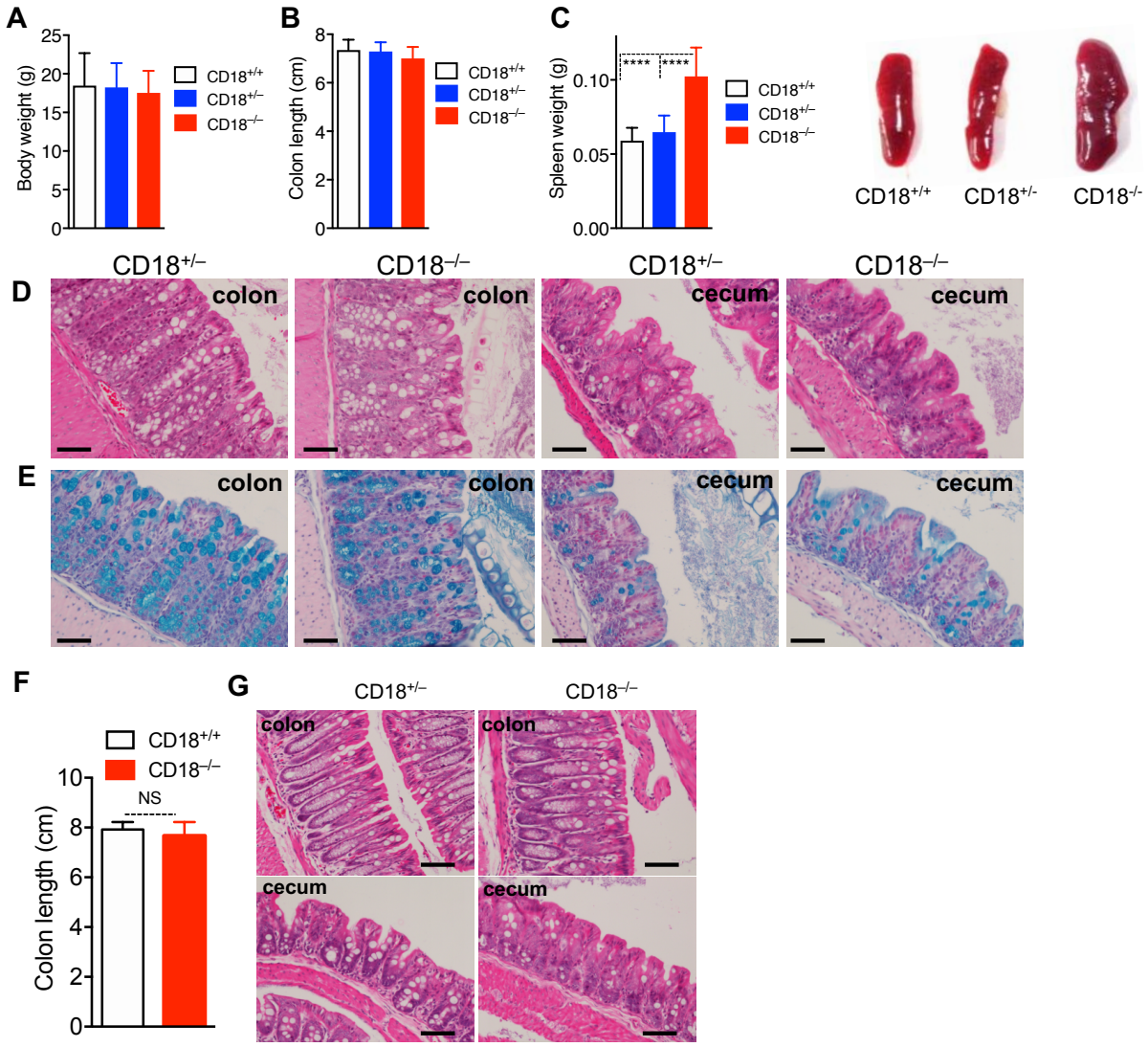

Figure S1: CD18-deficient mice do not exhibit intestinal pathology at steady state. Related to Figure 1.
(A-C) Eight-week-old CD18$^{-/-}$, CD18$^{+/-}$ and CD18$^{+/+}$ littermates were compared in terms of body weight (A), colon length (B), and spleen weight (left) and gross appearance of spleen (right) (C).
(D,E) Representative histological images of colon and cecum of the indicated mouse genotypes stained with H&E (D) or with Alcian blue which stains mucins in goblet cells (E). Scale bars, 50μm.
(F,G) Eighteen-week-old CD18$^{-/-}$ and CD18$^{+/+}$ littermates were compared for colon length (f) and histological appearance of colon and cecum tissue (G). Scale bars, 100μm.
Numerical data are means ± SD and are pooled from three independent experiments with three mice per group in two experiments and four mice per group in another experiment, for a total of ten mice per group (A-C,F). Images are representative of two independent experiments with three mice per group in each experiment (D,E,G). ****$P <$ 0.001 (one-way ANOVA with Tukey's multiple-comparisons test (A-C) or two-tailed Student's *t*-test (F)). NS, non-significant.

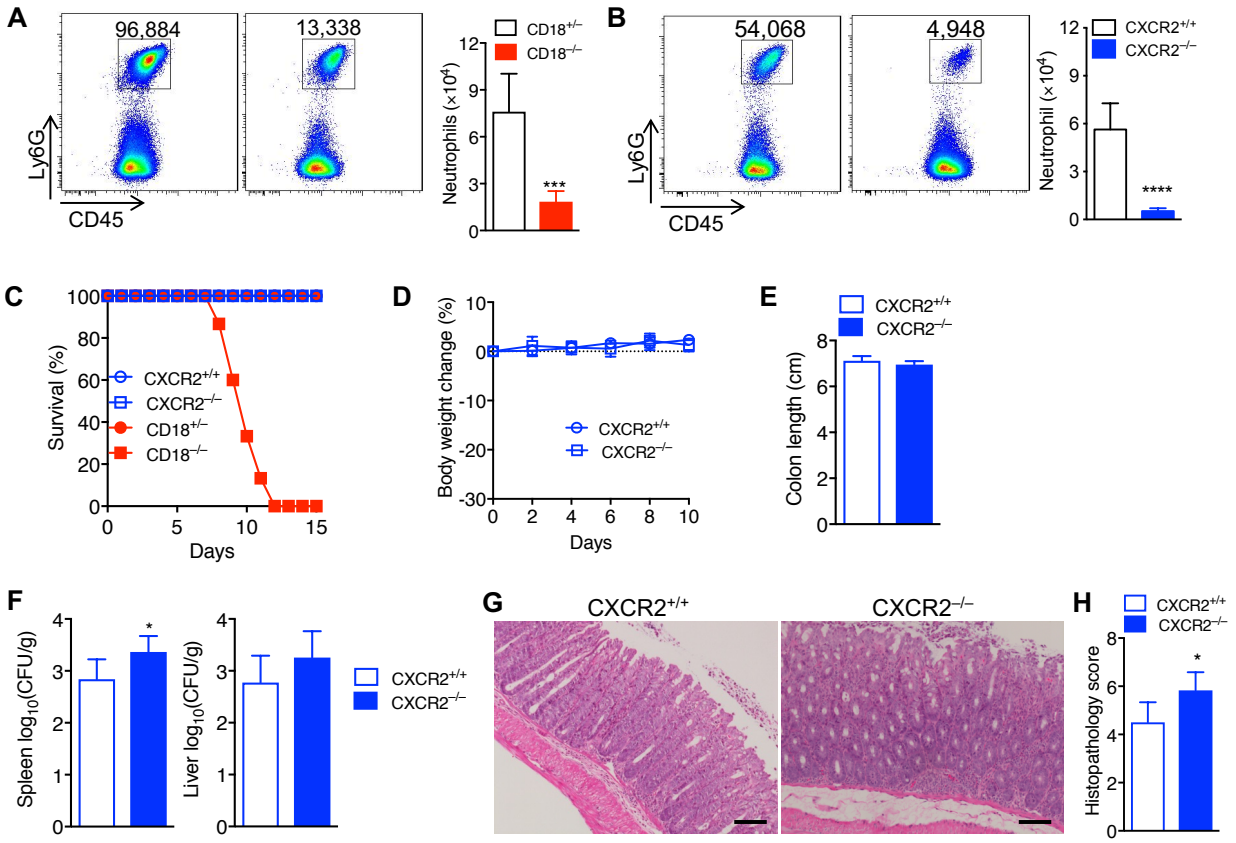

Figure S2: CXCR2 deficiency does not lead to acute lethality in *C. rodentium* infection. Related to Figure 1.
(A,B) Eight-week-old CD18$^{-/-}$ mice and CD18$^{+/-}$ littermate controls (A), or eight-week-old CXCR2$^{-/-}$ mice and CXCR2$^{+/+}$ littermate controls (B), were orally inoculated with *C. rodentium*. On day 8 post-infection, colonic LP cells were isolated and analyzed by flow cytometry for numbers of neutrophils (gated on CD45^{+}CD3^{-}B220^{-}F4/80^{-} Ly6G^{+}); FACS plots (left) and bar graph (right) showing absolute numbers of neutrophils.
(C-H) Eight-week-old CXCR2$^{-/-}$ and CXCR2$^{+/+}$ littermate controls, as well as CD18$^{-/-}$and CD18$^{+/-}$ littermate controls, were orally inoculated with *C. rodentium*. (C) Survival rates and (D) average weight changes at the indicated time points. At day 8 after inoculation, tissues were harvested and assayed for (E) colon length and (F) $\log_{10}$CFU of bacteria in spleen and liver. (G) Histological analysis of H&E-stained colon (scale bars, 100μm) and (H) histopathology scores of colon sections at day 8 post-infection.
Numerical data are means ± SD and are pooled from three independent experiments with two mice per group in each experiment, for a total of 6 mice per group (A,B); are from three independent experiments with five mice per group in each experiment, for a total of 15 mice per group (C); are from two independent experiments with three mice per group in each experiment, for a total of six mice per group (D,E); or are from three independent experiments with two mice per group in each experiment, for a total of six mice per group (F). Images are representative of three independent experiments with two mice per group in each experiment (G,H). *$P < 0.05$; ***$P < 0.001$ (two-tailed Student's *t*-test).

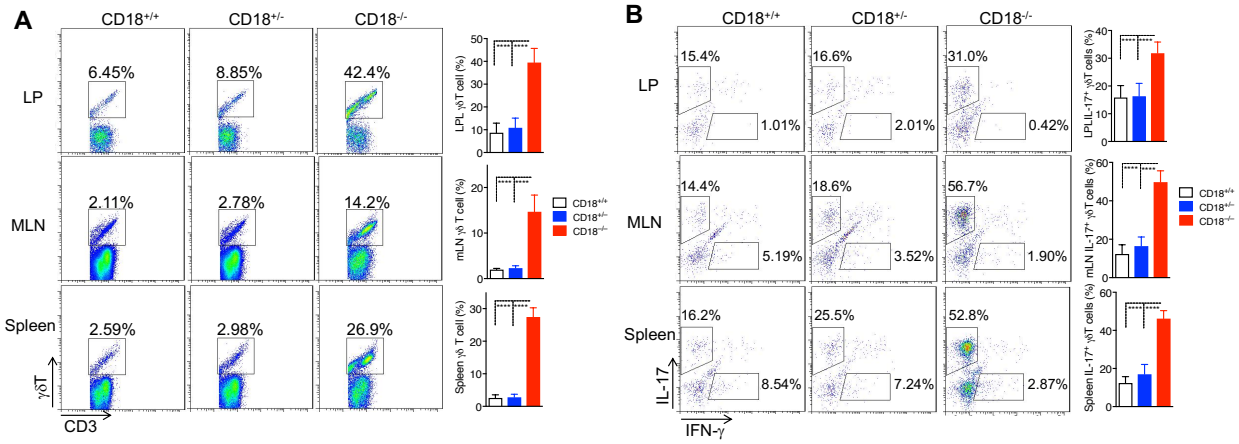

Figure S3: Elevated IL-17$^+$γδ T cells in CD18$^{-/-}$mice at steady state and after *C. rodentium* infection. Related to Figures 2 and 3.

(A,B) Eight-week-old CD18$^{-/-}$, CD18$^{+/-}$ and CD18$^{+/+}$ littermates were orally inoculated with *C. rodentium*. At day 8 post-inoculation, large intestine, MLN, and spleen were harvested and processed for flow cytometric analysis of frequency of γδT cells (gated on CD45$^+$CD3$^+$ cells) (A) and frequency of IL-17A$^+$ cells in γδ T cell population (B). (C,D) Large intestinal lamina propria (LP), MLN, and spleen were harvested from eight-week-old naïve CD18$^{-/-}$, CD18$^{+/-}$ and CD18$^{+/+}$ littermates and processed for flow cytometric analysis of frequency of γδT cells (gated on CD45$^+$CD3$^+$ cells) (C) and frequency of IL-17A$^+$ cells in γδ T cell population (D).

Numerical data are means ± SD. Data are representative of two independent experiments with three mice per group in one experiment and four mice in the other, for a total of seven mice per group (A,D) or are representative of two independent experiments with three or four mice per group, for a total of six to eight mice per group (B,C). ****P < 0.0001 (one-way ANOVA with Tukey's multiple-comparisons test).

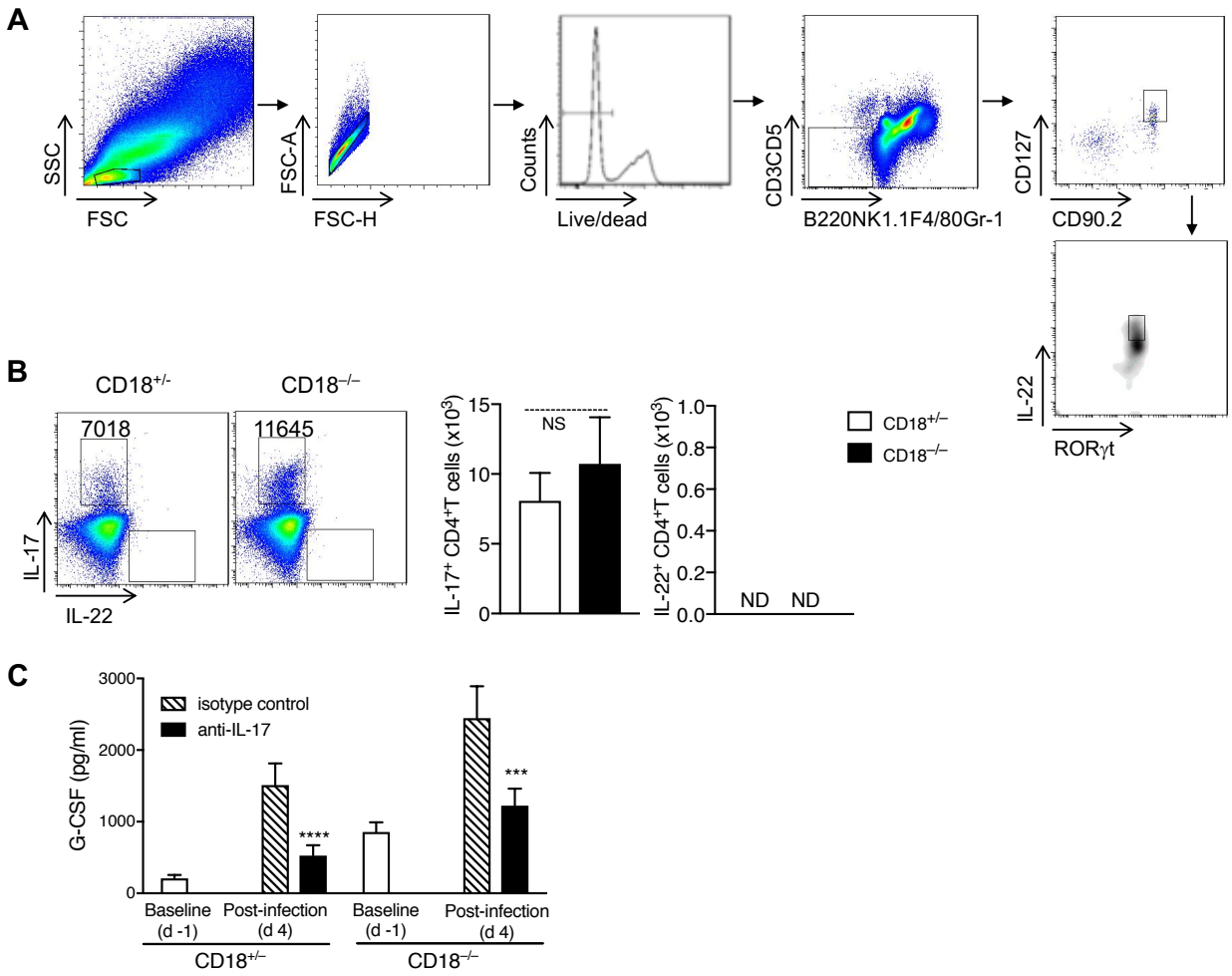

Figure S4: (A) Gating strategy for IL-22⁺ ILC3 detection. Related to Figures 2C, 3B, and 3D.
(B) Comparable numbers of intestinal IL-22⁺CD4⁺T cells in CD18$^{-/-}$ and CD18$^{+/-}$ mice. Related to Figure 2.
Eight-week-old CD18$^{-/-}$ mice and CD18$^{+/-}$ littermate controls were orally inoculated with *C. rodentium*. On day 8 post-infection, LPMCs were isolated from the large intestine and analyzed by flow cytometry; shown are FACS plots (left) and absolute numbers (right) of IL-22⁺CD4⁺T cells (gated on CD3⁺CD4⁺). Data are means ± SD and are pooled from two independent experiments with three mice per group in one experiment and two mice per group in the other experiment, for a total of five mice per group. NS, non-significant (two-tailed Student's *t*-test). ND, not detectable.
(C) Anti-IL-17 causes a decrease in the G-CSF levels in the serum of *C. rodentium*-infected mice. Related to Figure 3. Eight-week-old CD18$^{-/-}$ or CD18$^{+/+}$ littermates were orally inoculated with *C. rodentium*. Anti-IL-17 antibody was given on a daily basis starting 1 day before infection (d -1; baseline). Serum samples were obtained at baseline and day 4 post-infection (d 4) and serum G-CSF levels were measured by ELISA.
Numerical data represent means ± SD and are from two independent experiments each with three mice per group, for a total of six mice per group. ***$P < 0.001$; ****$P < 0.0001$ (two-tailed Student's *t*-test).

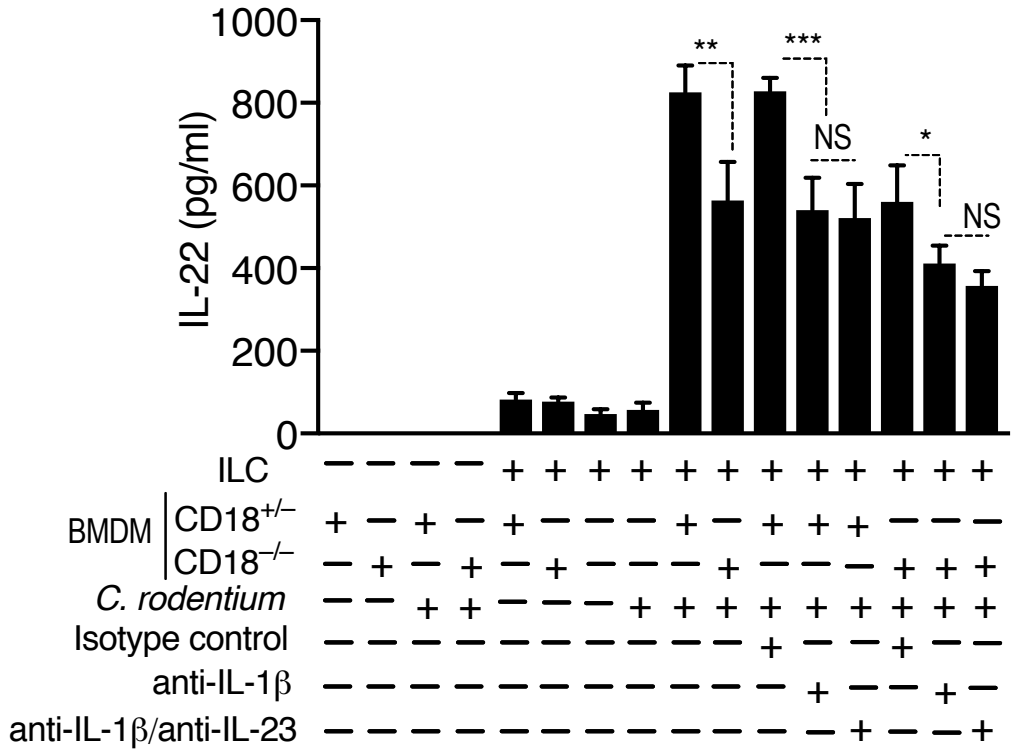

Figure S5: Importance of IL-1β and IL-23 for induction of IL-22 in *C. rodentium*-stimulated BMDM-ILC co-culture system. Related to Figure 5.

ILCs ($CD3^-CD5^-B220^-NK1.1^-F4/80^-Gr\text{-}1^-CD90^+CD127^+CD25^+KLRG1^-$) were sort-purified from the intestine of naïve $CD18^{-/-}$ mice. Sorted ILCs and BMDMs from naïve $CD18^{+/-}$ or $CD18^{-/-}$ mice were cultured alone or co-cultured, with or without stimulation with *C. rodentium* (MOI 20:1) for 24h, in the presence of anti-IL-1β, anti-IL-1β and anti-IL-23, or isotype control (IC). IL-22 was measured by ELISA of culture supernatants. Data are means ± SD and are pooled from two independent experiments performed in duplicate, for a total of four replicates (co-cultures) per group. ** $P < 0.01$ (two-tailed Student's *t*-test). NS, non-significant.

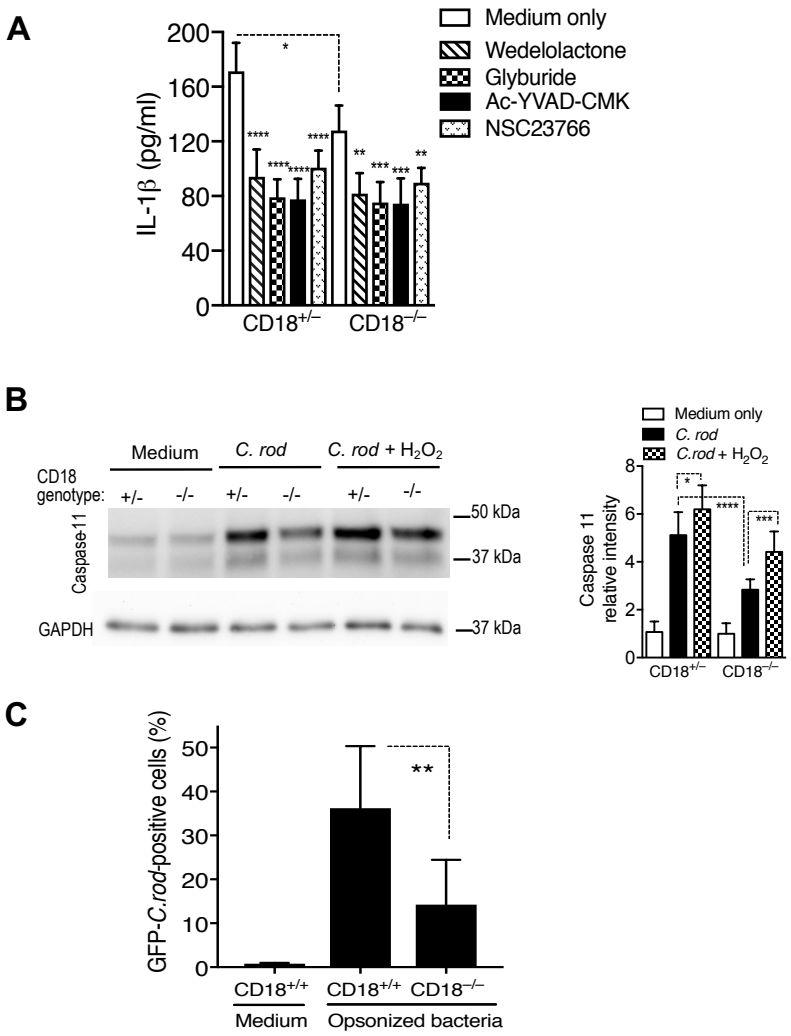

Figure S6: (A) IL-1β production by *C. rodentium*-stimulated intestinal macrophages is regulated by CD18, Rac1, and the inflammasome pathway. Related to Figure 6. $CD18^{+/-}$ and $CD18^{-/-}$ intestinal macrophages ($CD45^{+}Lin^{-}$ (CD3NK1.1B220Ly6G)$F4/80^{+}CX3CR1^{+}$) were pre-treated for 1h with the indicated inhibitors and then infected with *C. rodentium* for 24h. Supernatants were harvested and analyzed for IL-1β release by ELISA. Data are means ± SD and are pooled from two independent experiments performed in duplicate, for a total of four replicates (cell cultures) per group. $*P < 0.05$; $**P < 0.01$; $***P < 0.001$; $****P < 0.0001$ (one-way ANOVA with Dunnett's multiple comparisons test or two-tailed Student's *t*-test for comparing untreated $CD18^{+/-}$ and $CD18^{-/-}$ macrophages).
(B) H_2O_2 treatment restores caspase-11 expression in $CD18^{-/-}$ BMDMs. Related to Figure 6. $CD18^{+/-}$ and $CD18^{-/-}$ BMDMs were infected with *C. rodentium* at a MOI of 20:1 and after 6h were treated with 50 μM of H_2O_2 as a ROS source. After 2.5h, cell lysates were harvested and analyzed by immunoblotting with anti-mouse-caspase-11 antibody (left) and densitometry (right). Numerical data are means ± SD and are pooled from four independent experiments with two replicates per group for a total of eight replicates per group. $*P < 0.05$; $***P < 0.001$; $****P < 0.0001$ (two-tailed Student's *t*-test).
(C) Phagocytosis of *C. rodentium* by $CD18^{-/-}$ and $CD18^{+/+}$ BMDMs. Related to Figure 6. BMDMs were exposed to serum-opsonized GFP-*C. rodentium* (MOI 20:1) at 37°C for 30 mins to allow uptake of bacteria by the BMDMs. After BMDMs were treated with gentamycin to kill non-phagocytosed bacteria, they were stained with anti-mouse F4/80 antibody and phagocytic activity (% cells positive for GFP-*C. rodentium* [GFP-*C. rod*]) was assessed by flow cytometric analysis. Non-infected BMDMs were used as negative controls. Data are means ± SD and are pooled from three independent experiments for a total of seven to nine biological replicates per group. $**P < 0.01$ (two-tailed Student's *t*-test).